The Henryk Niewodniczański
INSTITUTE OF NUCLEAR PHYSICS
Ul. Radzikowskiego 152, 31-342 Kraków, Poland.

www.ifj.edu.pl/reports/reports.htm

Report No 1840/AP

The Monte Carlo calculated spectra and angular distributions of secondary particles from 3, 30 and 250 GeV electron interactions in thick Al, Cu, Nb and Pb targets.

D. Dworak, J. Łoskiewicz, H. Dinter, A. Leuschner and K. Tesch.

Kraków, January 2000.

20.XII.1999

The Monte Carlo calculated spectra and angular distributions of secondary particles from 3, 30 and 250 GeV electron interactions in thick Al, Cu, Nb and Pb targets.

D. Dworak and J. Loskiewicz, Institute of Nuclear Physics, Krakow, Poland
H. Dinter, A. Leuschner and K. Tesch, DESY, Hamburg, Germany

1. Introduction

The calculations were performed using the Monte Carlo code FLUKA (Fluka, 98). Its event generator is using the dual parton model and standard quantum chromodynamics (Ferrari, Sala, 1996), (Haenssen, Moehring, Ranft, 1984).
The calculations were performed mainly for shielding purposes. Therefore thick cylinder targets were chosen which give high neutron fluxes. Spectra of neutrons, protons, and charged pions are calculated since these hadrons give the most important contributions to total doses.

Aluminum, copper and niobium were used as target materials, which are frequently encountered in the vicinity of the internal beam. The same calculations were done also for lead (Pb) but the results are not appreciably different from those for niobium.

2. Calculations

The geometry assumed for the calculations is shown in Fig.1. This geometry allows to study the particle field around the target. The target was a thick cylinder, whose size varied with the target material and the primary energy. The size was chosen as to correspond to ~90% of neutron production in an infinitely thick target. The actual sizes of targets are shown in the Table 1.

The incident electron energy was 3, 30 and 250 GeV. Calculations for 1,10 and 100GeV were also performed but the results will not be shown in order to keep the size of the report within acceptable limits. The fluence spectra were calculated for the following emission angle ranges (in degrees): 0 –10, 10-20, 20-30, 30-40, 40-50, 50-60, 60-70, 70-80, 80-100, 100-120, 120-140, 140-160 and 160-180. The angles are in the laboratory frame. The following particles were tracked: neutrons, protons, charged pions and γ-rays.

To score the particle fluences (cosine weighted currents) the boundary crossing one-way fluence estimators were used. This expression means that each particle is scored as it crosses the given surface.

Table 1
Sizes of the targets for different materials and beam energies

Material	Target diameter [cm]	Target length in cm for beam energy in GeV					
		1	3	10	30	100	250
Al	**24.0**	**70**	**85**	**100**	**112**	**125**	**137**
Cu	**8.0**	**14**	**17**	**20**	**22**	**24**	**26**
Nb	**10.0**	**12**	**15**	**16**	**19**	**20**	**22**
Pb	**4.0**	**7**	**7**	**7**	**8**	**8**	**8**

All particles were scored on the surface of a sphere which surrounds the target positioned at its center and has an arbitrarily set radius of R= 500 cm. The whole sphere is subdivided into 13 detectors – spherical rings limited by two polar “theta” angles according to the angular ranges mentioned above. If any particle has crossed a given detector it was considered as emitted into the corresponding angular range (the point source approximation). Apparently, this approximation is good when the ratio of the radius R to the target dimensions is high. In the cases of Cu, Nb, and Pb these ratios are good enough (see Table 1). In case of long aluminum targets our assumptions can result in little misplacements of the particles in-between the detectors.

In the Table 2 below there are inserted the detector areas which were used to determine the final particle fluences.

In the version of the FLUKA code used, the hadrons are produced by the bremsstrahlung photons. Four types of photonuclear interactions producing hadrons are taken into account:

- production via Giant Dipole Resonance interactions
- production via quasi-deuteron interactions
- production in the region of the Delta resonance
- the other high-energy interactions (above 0.7 GeV).

To avoid very CPU time consuming histories we used the following energy cut-off values for the particle transport:

- neutrons: 1.0e-5 eV (thermal energies)
- protons: 1 MeV
- π^+, π^-: 1 MeV
- photons: 1 MeV
- e+, e-: 1 MeV
- other particles: 10 MeV.

Neutrinos and heavy ions interactions and transport are both not taken into account.

Table 2
The detectors and their areas

Detector	Theta range [deg]	Area [cm^2]
1	0- 10	23864
2	10- 20	70867
3	20- 30	115716
4	30- 40	157050
5	40- 50	193611
6	50- 60	224290
7	60- 70	248154
8	70- 80	264478
9	80-100	545532
10	100-120	512632
11	120-140	417902
12	140-160	272766
13	160-180	94731

3. Discussion of the results

The fluences integrated over the energy are shown in the Tables I, II and III for the beam energies 3, 30 and 250 GeV. Here the data for all angular intervals are presented.

Figures I to VI include the energy distributions. All spectra are normalized to unity, i.e. the area under each curve on the log scale is equal to one. In such a way the direct comparison of the curve shapes is possible.

In Fig. I.1 to III.6 the neutron, proton and charged pion fluences are plotted as a function of the particle energy. In each figure these three spectra are plotted for the same incident energy and production angle. On the same sheet of paper are collected the data for the four target materials – aluminum, copper, niobium and lead. The neutron spectra are showing the typical two-modal distribution (Gorbatkov, 1994, Dinter et al, 1996). The lower energy peak around 1 MeV is known to come from the evaporation process, and the higher energy peak around 100 MeV comprises intranuclear cascade hadrons. This second peak has a marked tendency to diminish with increasing target atomic number. Also with increasing emission angle its size is shrinking. The proton and charged pion spectra, which at small angles differ in the average energy, are coming nearer to each other as the emission angle grows. This behavior is present at all energies. The spectra are shown for the angular ranges 10-20, 20-30,40-50,60-70, 80-100 and 140-160 degrees.

The next set of figures is showing the comparison of fluence spectra for different incident energies, particles and targets. In Fig. IV.1 are shown the neutron spectra from the Al target for all three energies and two angular ranges. It is evident that the shapes of the spectra are quite similar. The Fig. IV.2 shows the same behavior but here the target is copper. Also for niobium and lead the neutron spectrum shape depends even less on the incident energy. This can be seen in the Figs. IV.3 and IV.4.

For secondary protons and charged pions there is an apparent incident energy effect, the modal value of the distribution is shifted towards higher energies by approximately a factor of two between 3 and 30 GeV and somewhat less between 30 and 250 GeV. This effect is less marked for heavier targets and in backward direction. These results can be looked at in Fig. V.1 to VI.4.

A more elaborate analysis will be published later.

Acknowledgements

This calculations were performed at ACK CYFRONET AGH, Cracow, according to grant no. KBN/SPP/IFJ/065/1998 and KBN/S2000/IFJ/065/1998.

Literature

1. A.Fasso,A.Ferrari,P.Sala,J.Ranft, FLUKA-98 (User Manual)
2. A.Ferrari,P.Sala, The Physics of High Energy Reactions, in Proceedings of the Workshop on Nuclear Reaction Data and Nuclear Reactors Physics, International Centre for Theoretical Physics, Trieste, Italy (1996)
3. K.Hanssen,H-J.Mohring,J.Ranft, Hadronic event generation for hadron cascade calculations and detector simulation II. Inelastic hadron-nucleus collisions at energies below 5 GeV Nucl.Sci.Eng. 88 (1984) 551
4. D.V.Gorbatkov and Kryuchkov, Part.Accel.Conf., London 1994 and IHEP Report 94-47 Protvino 1994
5. H.Dinter,K.Tesch,D.Dworak, Studies on the neutron field behind shielding of proton accelerators Part I: Concrete shielding, NIM A 368 (1996) 265-272

Fig.1 Geometry of the problem

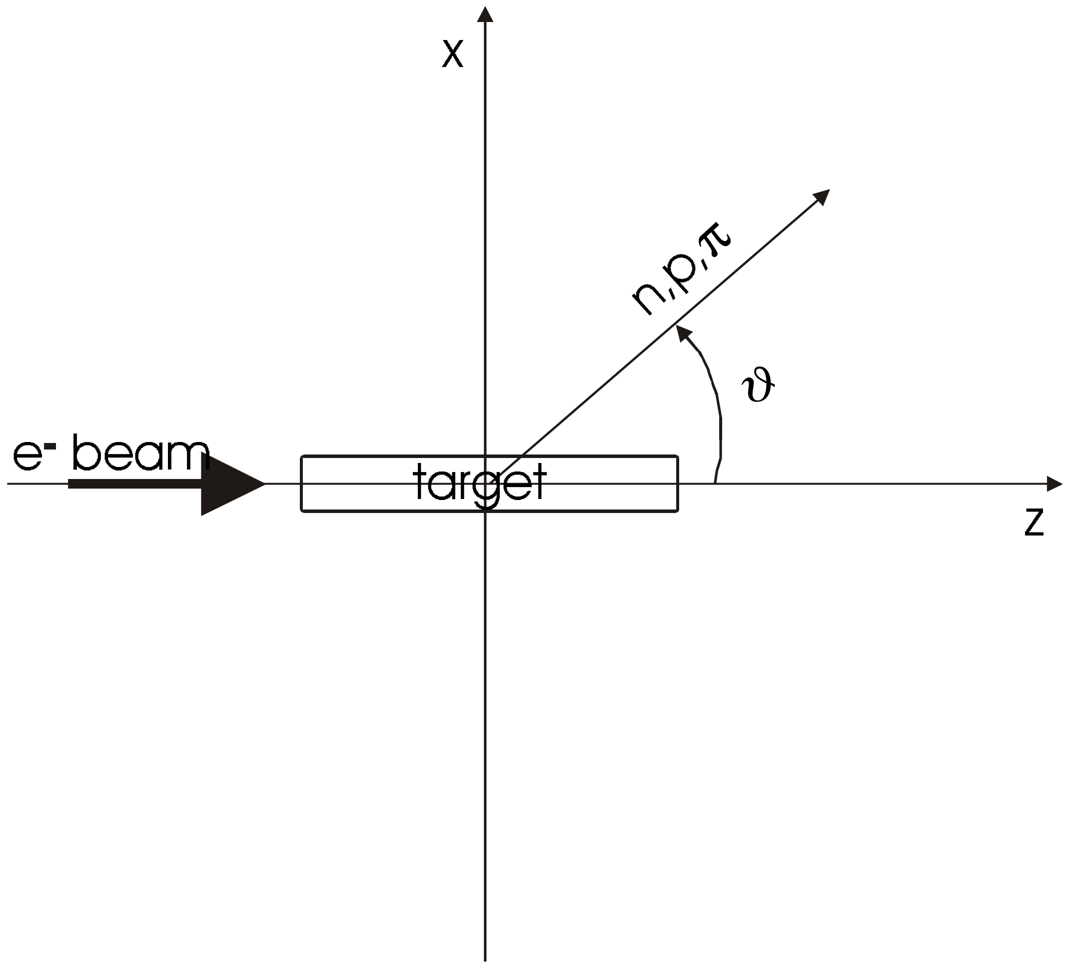

Table I

ABSOLUTE FLUENCE boundary crossing on-way ESTIMATORS
at R= 5 m (particles/cm2/beam electron)**

Energy of the electron beam: 3 GeV

****

Theta (deg)	Al target Neutr.	Al target Prot.	Al target Pi+-	Al target Gamma	Nb target Neutr.	Nb target Prot.	Nb target Pi+-	Nb target Gamma
0- 10	2.44-08	6.92-10	1.69-09	2.69-04	1.72-07	7.10-10	1.88-09	3.16-04
10- 20	3.29-08	8.49-10	1.78-09	6.66-05	1.79-07	5.26-10	1.19-09	1.09-04
20- 30	4.67-08	1.10-09	1.95-09	4.05-05	1.91-07	3.86-10	7.41-10	5.51-05
30- 40	6.08-08	9.89-10	1.75-09	2.83-05	2.11-07	3.45-10	5.80-10	3.60-05
40- 50	7.31-08	8.59-10	1.37-09	1.92-05	2.37-07	2.81-10	4.71-10	2.66-05
50- 60	8.39-08	6.90-10	1.05-09	1.20-05	2.62-07	2.34-10	3.63-10	1.97-05
60- 70	9.14-08	5.55-10	8.27-10	6.80-06	2.81-07	1.92-10	2.68-10	1.44-05
70- 80	9.60-08	4.34-10	6.19-10	3.84-06	2.93-07	1.59-10	1.97-10	1.05-05
80-100	9.74-08	3.32-10	4.62-10	1.87-06	2.96-07	1.19-10	1.61-10	6.66-06
100-120	9.07-08	2.32-10	3.41-10	8.58-07	2.85-07	1.27-10	1.36-10	3.73-06
120-140	7.32-08	1.59-10	2.29-10	4.37-07	2.55-07	1.80-10	1.39-10	2.14-06
140-160	4.95-08	1.31-10	1.59-10	2.01-07	2.24-07	2.69-10	1.66-10	1.47-06
160-180	3.03-08	1.38-10	1.50-10	9.68-08	2.09-07	2.81-10	1.73-10	1.38-06
0-180	7.82-08	4.29-10	6.73-10	9.89-06	2.61-07	2.09-10	2.78-10	1.60-05

2.44-08 should be read as $2.44*10^{-8}$

Theta (deg)	Cu target Neutr.	Cu target Prot.	Cu target Pi+-	Cu target Gamma	Pb target Neutr.	Pb target Prot.	Pb target Pi+-	Pb target Gamma
0- 10	6.92-08	6.56-10	1.94-09	3.06-04	2.32-07	7.86-10	1.65-09	5.71-04
10- 20	7.51-08	5.92-10	1.35-09	9.65-05	2.31-07	6.71-10	1.13-09	1.93-04
20- 30	8.98-08	6.04-10	1.09-09	5.41-05	2.38-07	5.64-10	7.32-10	1.06-04
30- 40	1.09-07	5.63-10	8.83-10	3.99-05	2.55-07	5.41-10	5.26-10	7.68-05
40- 50	1.26-07	4.86-10	6.78-10	2.96-05	2.71-07	4.93-10	4.00-10	5.84-05
50- 60	1.41-07	3.84-10	5.38-10	2.09-05	2.83-07	4.13-10	3.00-10	4.40-05
60- 70	1.51-07	3.13-10	3.75-10	1.41-05	2.91-07	3.49-10	2.34-10	3.32-05
70- 80	1.57-07	2.58-10	3.11-10	9.53-06	2.94-07	3.12-10	2.01-10	2.56-05
80-100	1.59-07	2.10-10	2.37-10	5.62-06	2.95-07	2.64-10	1.69-10	1.80-05
100-120	1.51-07	1.61-10	1.77-10	2.98-06	2.89-07	2.67-10	1.50-10	1.18-05
120-140	1.31-07	1.73-10	1.56-10	1.59-06	2.70-07	2.87-10	1.55-10	7.71-06
140-160	1.04-07	2.13-10	1.63-10	8.41-07	2.43-07	3.46-10	1.62-10	5.09-06
160-180	8.54-08	2.41-10	1.69-10	6.14-07	2.29-07	3.78-10	1.85-10	4.29-06
0-180	1.35-07	2.84-10	3.76-10	1.55-05	2.75-07	3.52-10	2.67-10	3.46-05

„0-180 deg" – average values over the whole sphere R=500 cm

Table II

ABSOLUTE FLUENCE boundary crossing one-way ESTIMATORS at R= 5 m (particles/cm2/beam electron)**

Energy of the electron beam: 30 GeV

****

	Al target				Nb target			
Theta (deg)	Neutr.	Prot.	Pi+-	Gamma	Neutr.	Prot.	Pi+-	Gamma
0- 10	2.50-07	1.58-08	6.19-08	2.54-03	1.49-06	1.17-08	6.01-08	2.67-03
10- 20	3.59-07	1.87-08	4.86-08	6.27-04	1.62-06	8.79-09	2.49-08	8.97-04
20- 30	5.14-07	2.05-08	4.06-08	4.00-04	1.82-06	6.89-09	1.44-08	4.78-04
30- 40	6.64-07	1.77-08	3.04-08	2.81-04	2.12-06	5.63-09	1.02-08	3.38-04
40- 50	7.97-07	1.39-08	2.25-08	1.90-04	2.45-06	4.48-09	7.36-09	2.61-04
50- 60	9.05-07	1.06-08	1.63-08	1.18-04	2.76-06	3.52-09	5.29-09	1.97-04
60- 70	9.74-07	8.06-09	1.20-08	6.63-05	2.99-06	2.80-09	3.84-09	1.45-04
70- 80	1.02-06	6.20-09	9.01-09	3.73-05	3.14-06	2.26-09	2.86-09	1.05-04
80-100	1.03-06	4.32-09	6.42-09	1.82-05	3.19-06	1.63-09	2.04-09	6.70-05
100-120	9.42-07	2.64-09	4.29-09	8.39-06	3.00-06	1.09-09	1.42-09	3.72-05
120-140	7.34-07	1.46-09	2.61-09	4.24-06	2.49-06	8.87-10	1.05-09	1.96-05
140-160	4.42-07	7.74-10	1.31-09	1.82-06	1.85-06	9.48-10	9.57-10	9.91-06
160-180	1.91-07	4.69-10	7.05-10	5.56-07	1.45-06	1.04-09	9.76-10	7.69-06
0-180	8.13-07	6.41-09	1.11-08	9.59-05	2.65-06	2.45-09	4.27-09	1.47-04

	Cu target				Pb target			
Theta (deg)	Neutr.	Prot.	Pi+-	Gamma	Neutr.	Prot.	Pi+-	Gamma
0- 10	5.98-07	1.25-08	6.31-08	2.53-03	2.31-06	1.40-08	5.54-08	6.91-03
10- 20	7.04-07	1.09-08	2.98-08	7.93-04	2.32-06	1.11-08	2.31-08	2.14-03
20- 30	8.96-07	1.05-08	2.10-08	4.95-04	2.38-06	8.89-09	1.27-08	1.14-03
30- 40	1.13-06	8.96-09	1.50-08	3.88-04	2.54-06	7.49-09	8.27-09	7.82-04
40- 50	1.33-06	7.24-09	1.08-08	2.95-04	2.67-06	6.30-09	5.74-09	5.78-04
50- 60	1.49-06	5.71-09	7.73-09	2.10-04	2.78-06	5.30-09	4.14-09	4.29-04
60- 70	1.60-06	4.51-09	5.65-09	1.42-04	2.85-06	4.43-09	3.11-09	3.20-04
70- 80	1.67-06	3.62-09	4.31-09	9.58-05	2.87-06	3.88-09	2.50-09	2.46-04
80-100	1.69-06	2.62-09	3.11-09	5.64-05	2.88-06	3.19-09	2.02-09	1.73-04
100-120	1.59-06	1.69-09	2.13-09	2.98-05	2.80-06	2.57-09	1.69-09	1.13-04
120-140	1.33-06	1.06-09	1.42-09	1.56-05	2.58-06	2.00-09	1.39-09	7.18-05
140-160	9.14-07	8.19-10	9.73-10	6.83-06	2.18-06	1.71-09	1.14-09	4.04-05
160-180	5.84-07	7.75-10	8.27-10	3.42-06	1.87-06	1.82-09	1.16-09	2.69-05
0-180	1.39-06	3.66-09	5.89-09	1.45-04	2.66-06	3.94-09	3.87-09	3.56-04

Table III

ABSOLUTE FLUENCE boundary crossing one-way ESTIMATORS at R= 5 m (particles/cm2/beam electron)**

Energy of the electron beam: 250 GeV

****

Theta (deg)	Al target Neutr.	Al target Prot.	Al target Pi+-	Al target Gamma	Nb target Neutr.	Nb target Prot.	Nb target Pi+-	Nb target Gamma
0- 10	2.16-06	1.94-07	8.45-07	1.97-02	1.20-05	1.32-07	7.37-07	2.23-02
10- 20	3.16-06	2.16-07	5.71-07	4.95-03	1.32-05	9.17-08	2.60-07	7.23-03
20- 30	4.54-06	2.17-07	4.40-07	3.30-03	1.51-05	6.97-08	1.47-07	3.88-03
30- 40	5.84-06	1.82-07	3.13-07	2.33-03	1.78-05	5.49-08	9.93-08	2.79-03
40- 50	6.96-06	1.38-07	2.22-07	1.57-03	2.08-05	4.32-08	6.99-08	2.17-03
50- 60	7.85-06	1.04-07	1.59-07	9.61-04	2.35-05	3.37-08	4.96-08	1.64-03
60- 70	8.46-06	7.75-08	1.14-07	5.38-04	2.55-05	2.63-08	3.54-08	1.20-03
70- 80	8.76-06	5.82-08	8.53-08	3.05-04	2.68-05	2.06-08	2.70-08	8.81-04
80-100	8.76-06	3.98-08	6.01-08	1.48-04	2.72-05	1.48-08	1.86-08	5.53-04
100-120	7.92-06	2.40-08	3.89-08	6.85-05	2.54-05	9.05-09	1.22-08	3.09-04
120-140	6.10-06	1.27-08	2.32-08	3.43-05	2.03-05	5.16-09	7.86-09	1.59-04
140-160	3.53-06	5.86-09	1.04-08	1.49-05	1.35-05	3.80-09	5.08-09	6.61-05
160-180	1.24-06	2.39-09	3.35-09	3.70-06	8.65-06	3.57-09	4.65-09	3.81-05
0-180	6.91-06	6.35-08	1.13-07	7.75-04	2.21-05	2.24-08	4.16-08	1.21-03

Theta (deg)	Cu target Neutr.	Cu target Prot.	Cu target Pi+-	Cu target Gamma	Pb target Neutr.	Pb target Prot.	Pb target Pi+-	Pb target Gamma
0- 10	4.78-06	1.43-07	7.84-07	2.02-02	1.85-05	1.72-07	6.74-07	8.61-02
10- 20	5.75-06	1.15-07	3.25-07	6.20-03	1.86-05	1.28-07	2.34-07	2.26-02
20- 30	7.57-06	1.05-07	2.15-07	4.03-03	1.86-05	9.41-08	1.20-07	1.09-02
30- 40	9.52-06	8.87-08	1.49-07	3.20-03	1.91-05	7.33-08	7.41-08	6.63-03
40- 50	1.13-05	7.02-08	1.05-07	2.44-03	1.97-05	5.83-08	5.11-08	4.52-03
50- 60	1.26-05	5.45-08	7.37-08	1.74-03	2.02-05	4.77-08	3.64-08	3.21-03
60- 70	1.36-05	4.22-08	5.35-08	1.18-03	2.05-05	3.91-08	2.67-08	2.34-03
70- 80	1.42-05	3.36-08	3.99-08	7.96-04	2.06-05	3.40-08	2.13-08	1.78-03
80-100	1.44-05	2.40-08	2.82-08	4.70-04	2.04-05	2.67-08	1.69-08	1.24-03
100-120	1.35-05	1.46-08	1.91-08	2.47-04	1.98-05	2.07-08	1.37-08	8.07-04
120-140	1.10-05	8.00-09	1.18-08	1.30-04	1.83-05	1.38-08	1.08-08	5.12-04
140-160	7.09-06	4.03-09	6.07-09	5.24-05	1.49-05	8.20-09	7.31-09	2.63-04
160-180	3.60-06	2.82-09	3.82-09	1.76-05	1.17-05	7.53-09	6.36-09	1.40-04
0-180	1.17-05	3.44-08	5.82-08	1.18-03	1.91-05	3.51-08	3.56-08	3.18-03

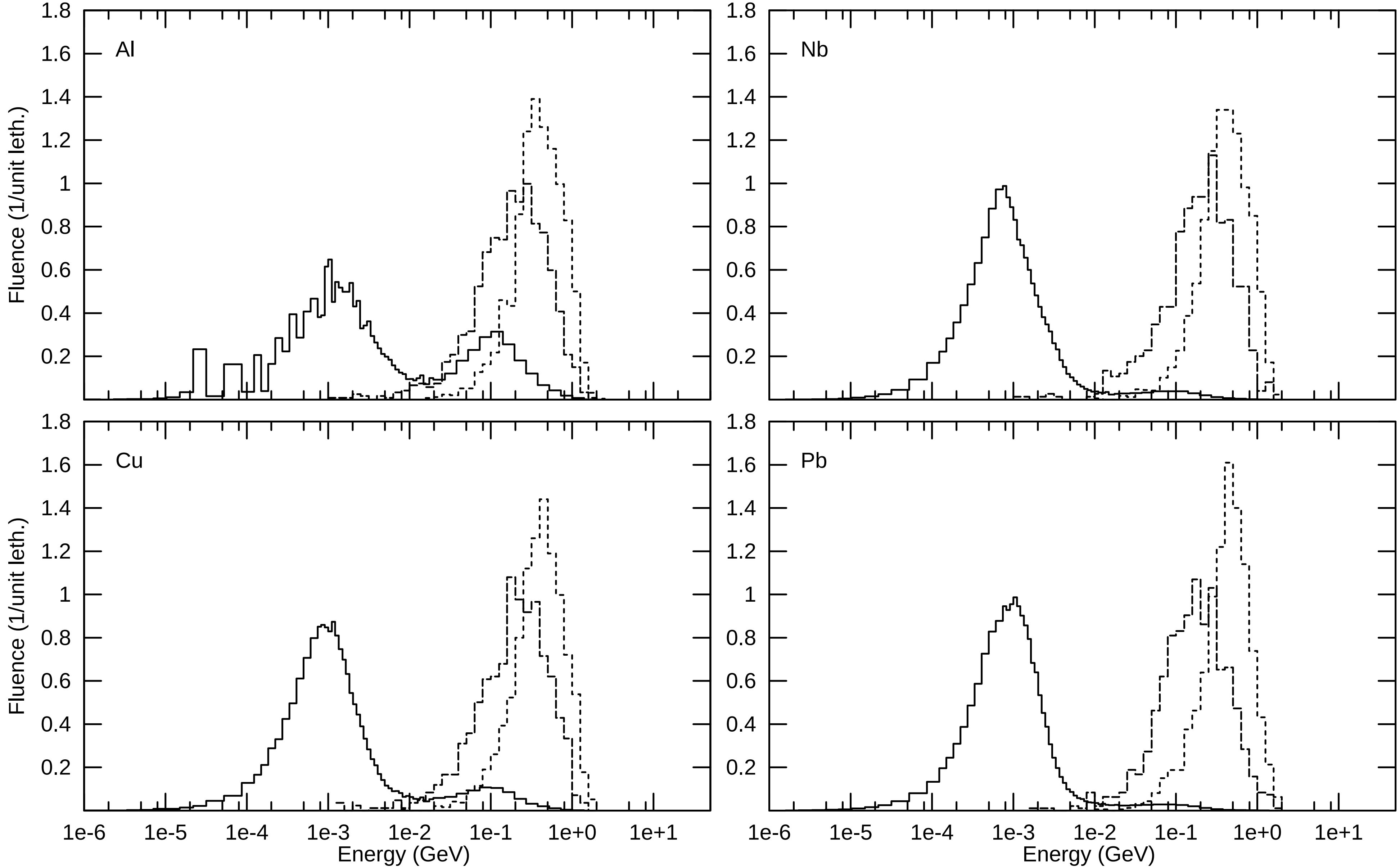

Fig. I.1: 3 GeV electron beam, Theta angle interval 10-20 deg
LINES: continuous - Neutrons, dashed - Protons, dotted - Charged pions

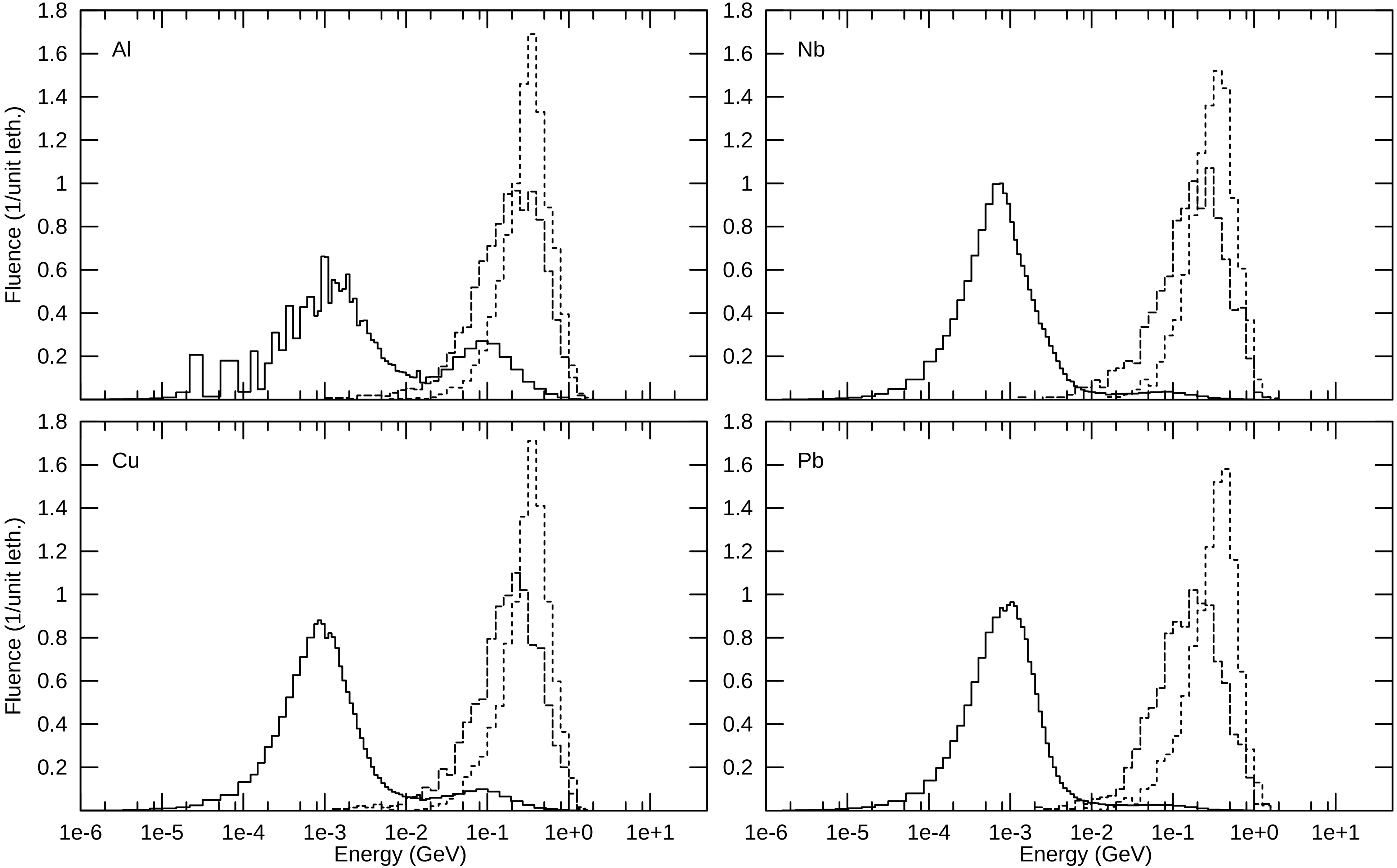

Fig. I.2: 3 GeV electron beam, Theta angle interval 20-30 deg
LINES: continuous - Neutrons, dashed - Protons, dotted - Charged pions

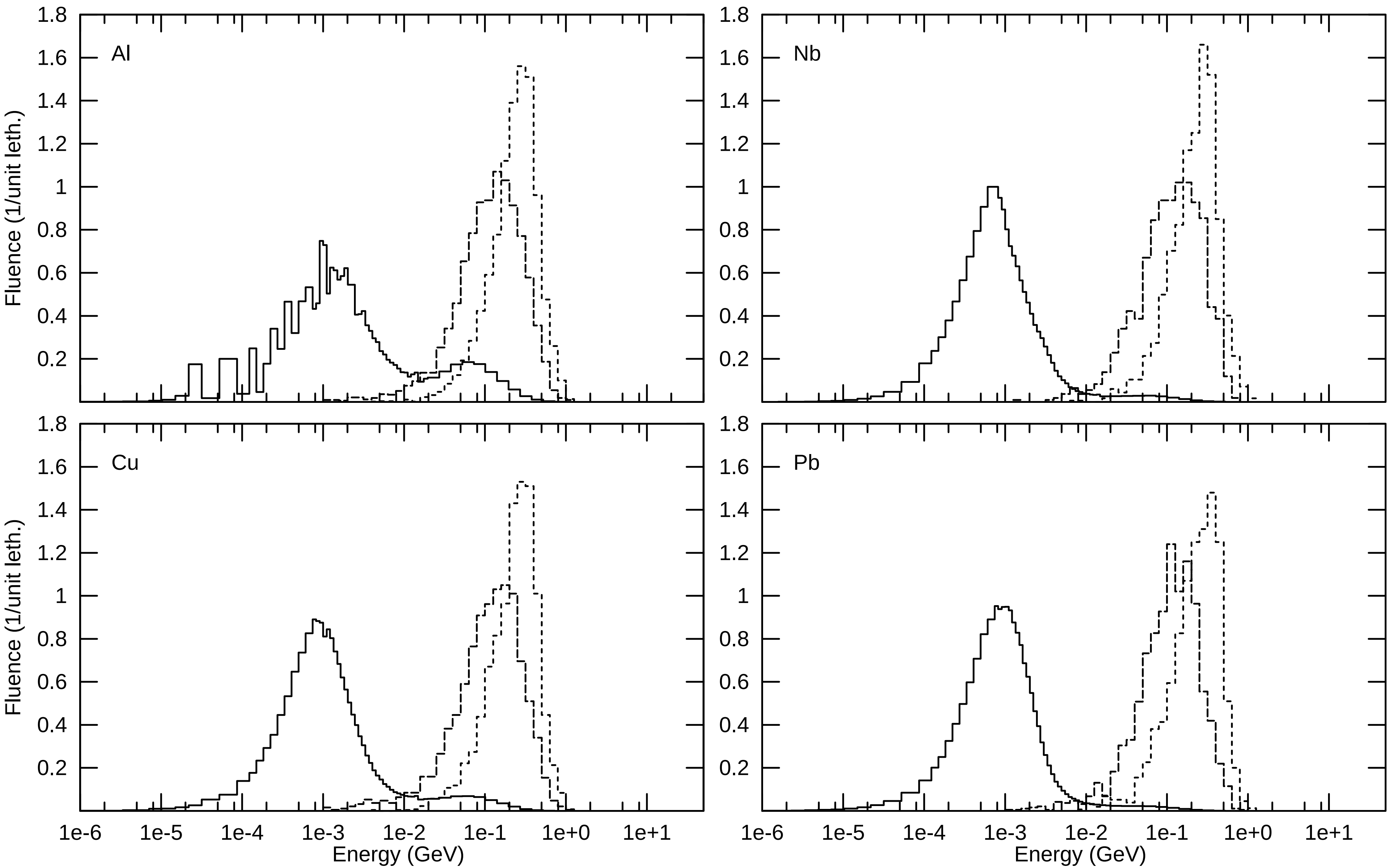

Fig. I.3: 3 GeV electron beam, Theta angle interval 40-50 deg

LINES: continuous - Neutrons, dashed - Protons, dotted - Charged pions

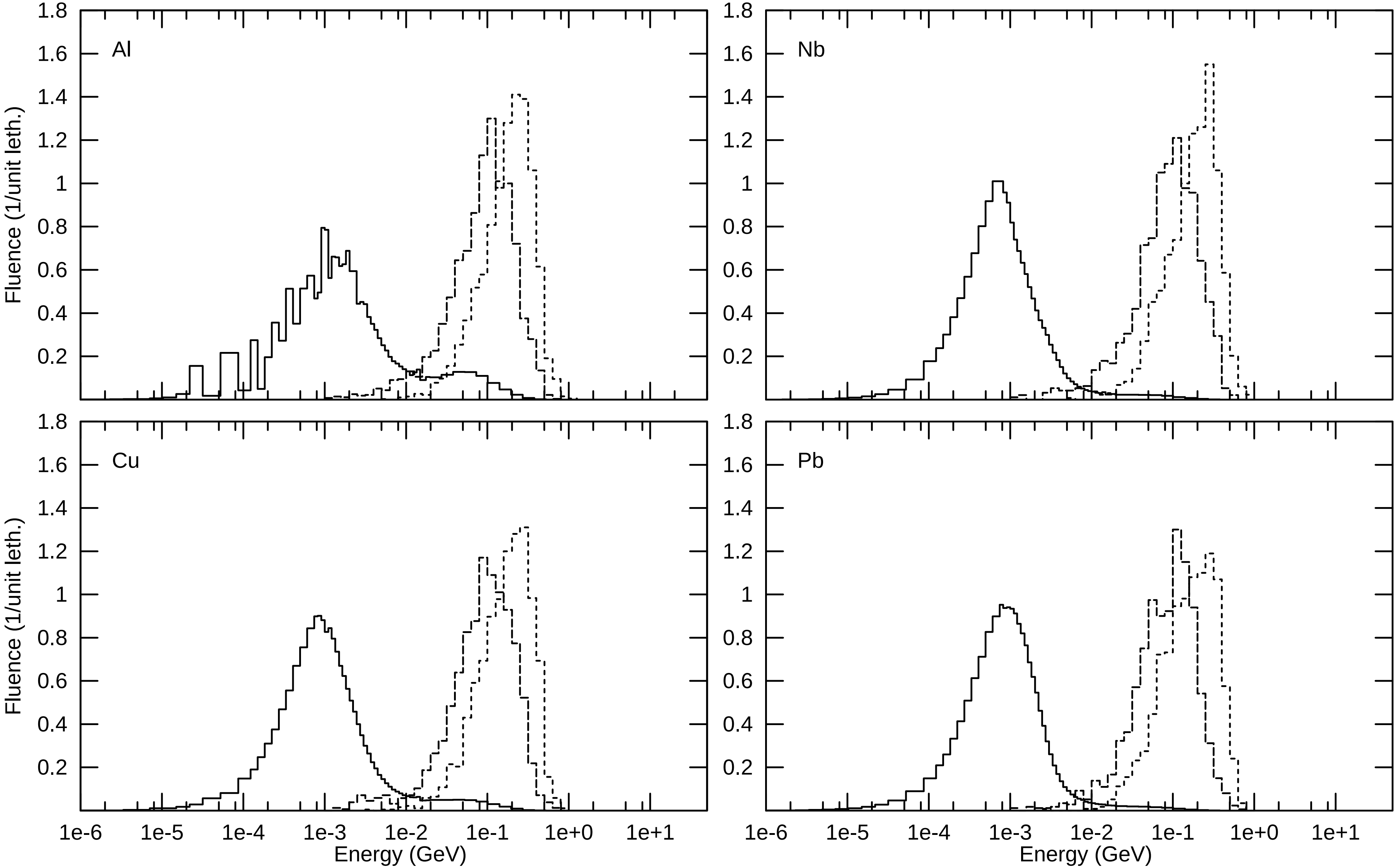

Fig. I.4: 3 GeV electron beam, Theta angle interval 60-70 deg
LINES: continuous - Neutrons, dashed - Protons, dotted - Charged pions

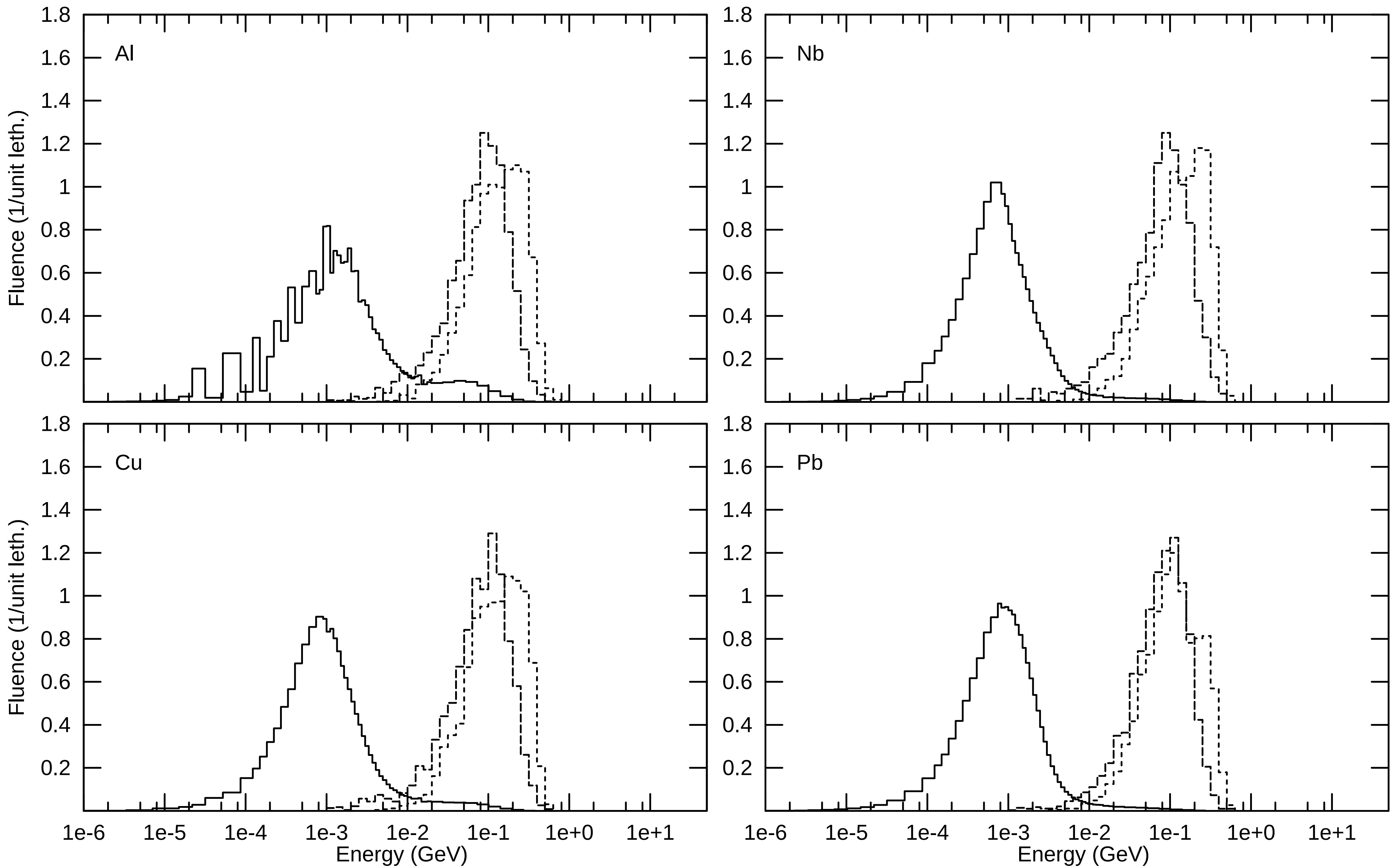

Fig. I.5: 3 GeV electron beam, Theta angle interval 80-100 deg
LINES: continuous - Neutrons, dashed - Protons, dotted - Charged pions

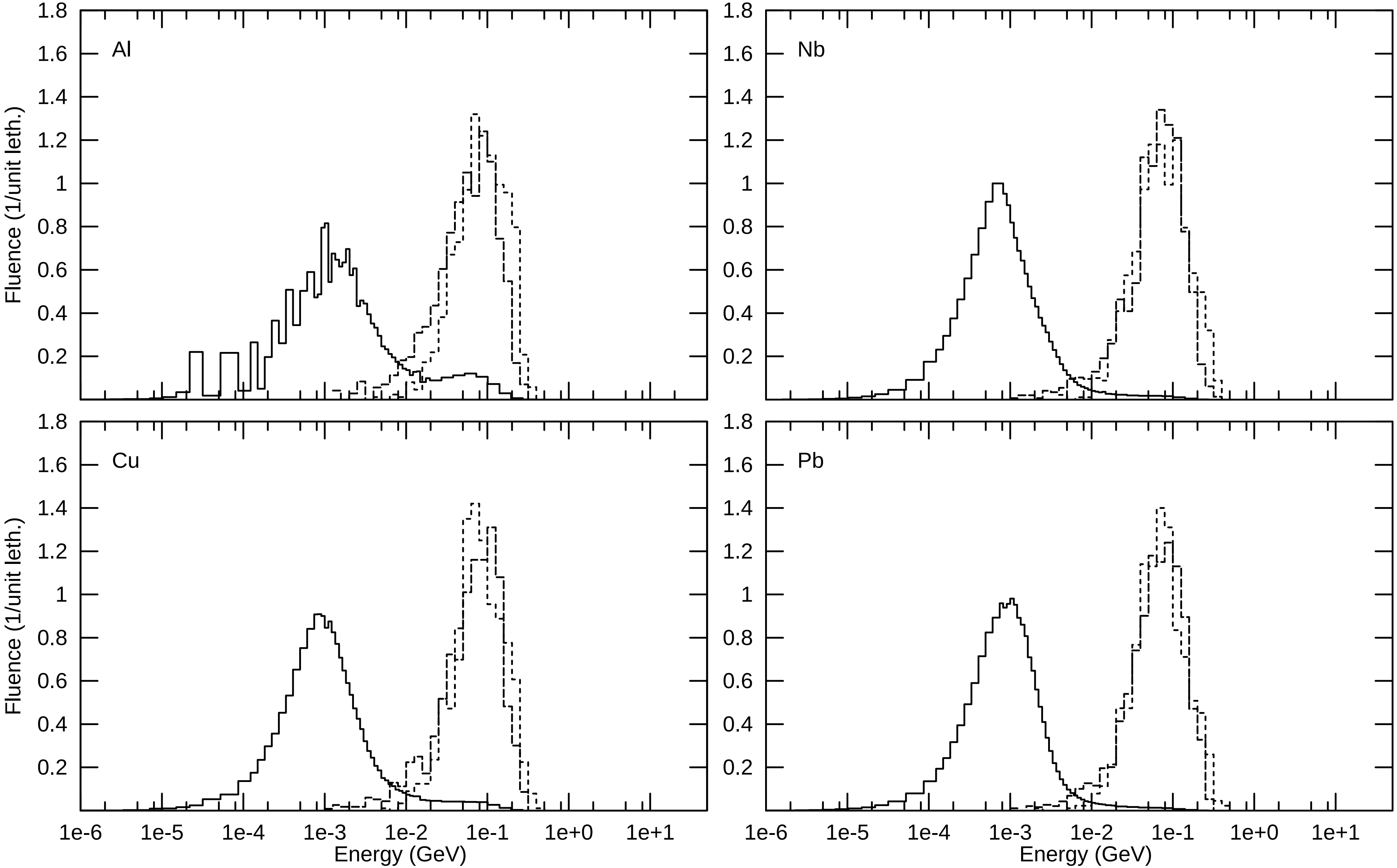

Fig. I.6: 3 GeV electron beam, Theta angle interval 140-160 deg
LINES: continuous - Neutrons, dashed - Protons, dotted - Charged pions

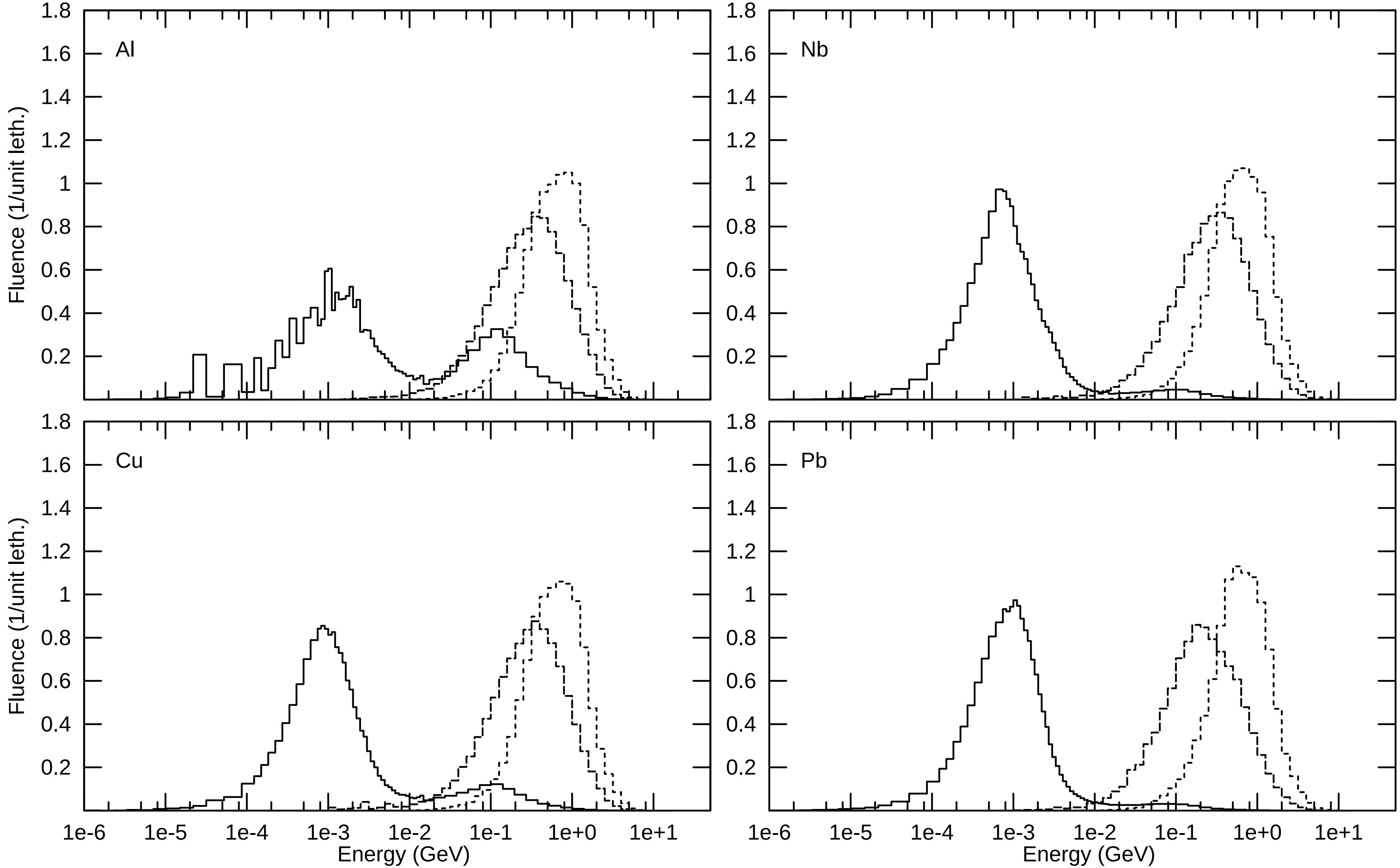

Fig. II.1: 30 GeV electron beam, Theta angle interval 10-20 deg

LINES: continuous - Neutrons, dashed - Protons, dotted - Charged pions

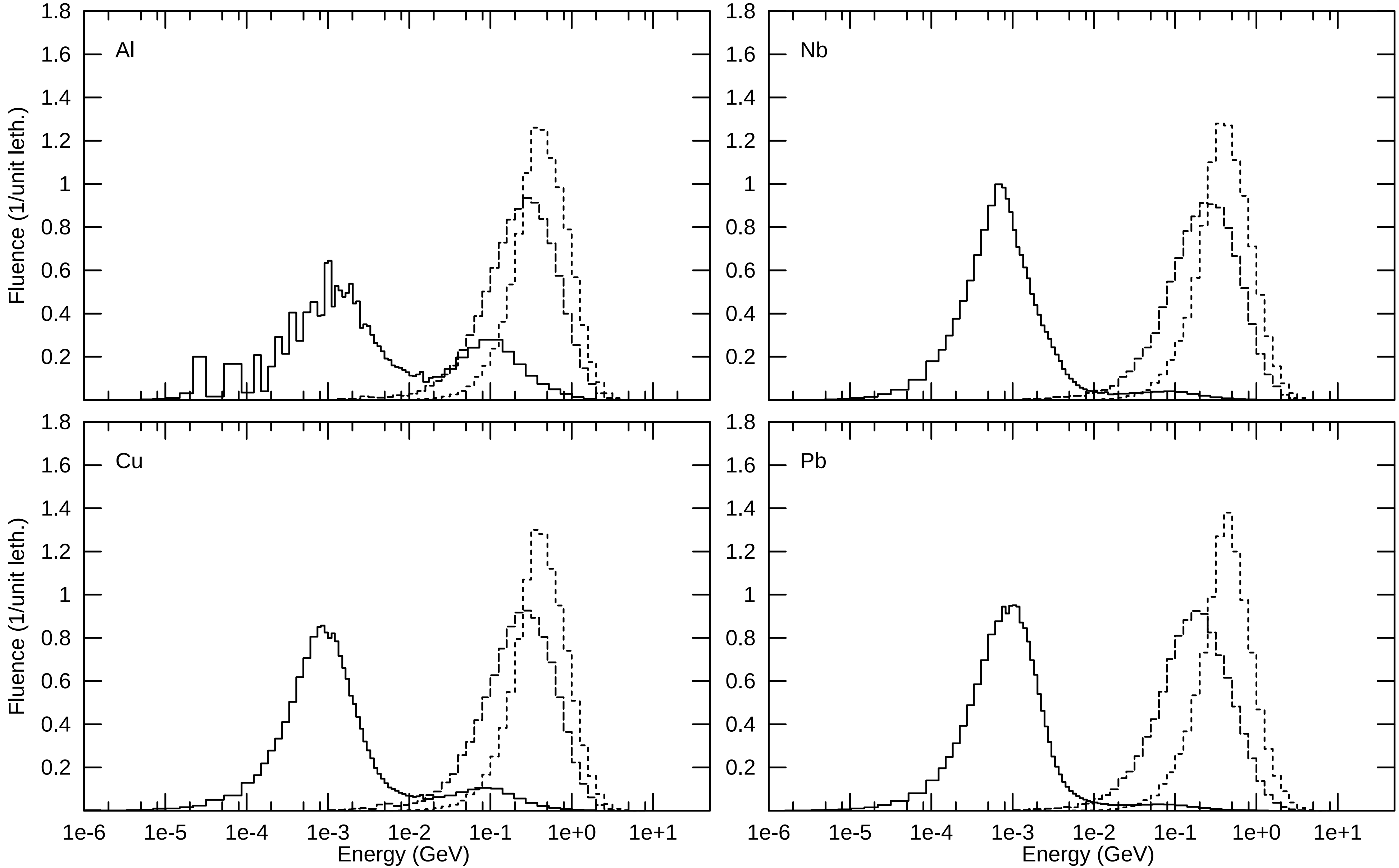

Fig. II.2: 30 GeV electron beam, Theta angle interval 20-30 deg
LINES: continuous - Neutrons, dashed - Protons, dotted - Charged pions

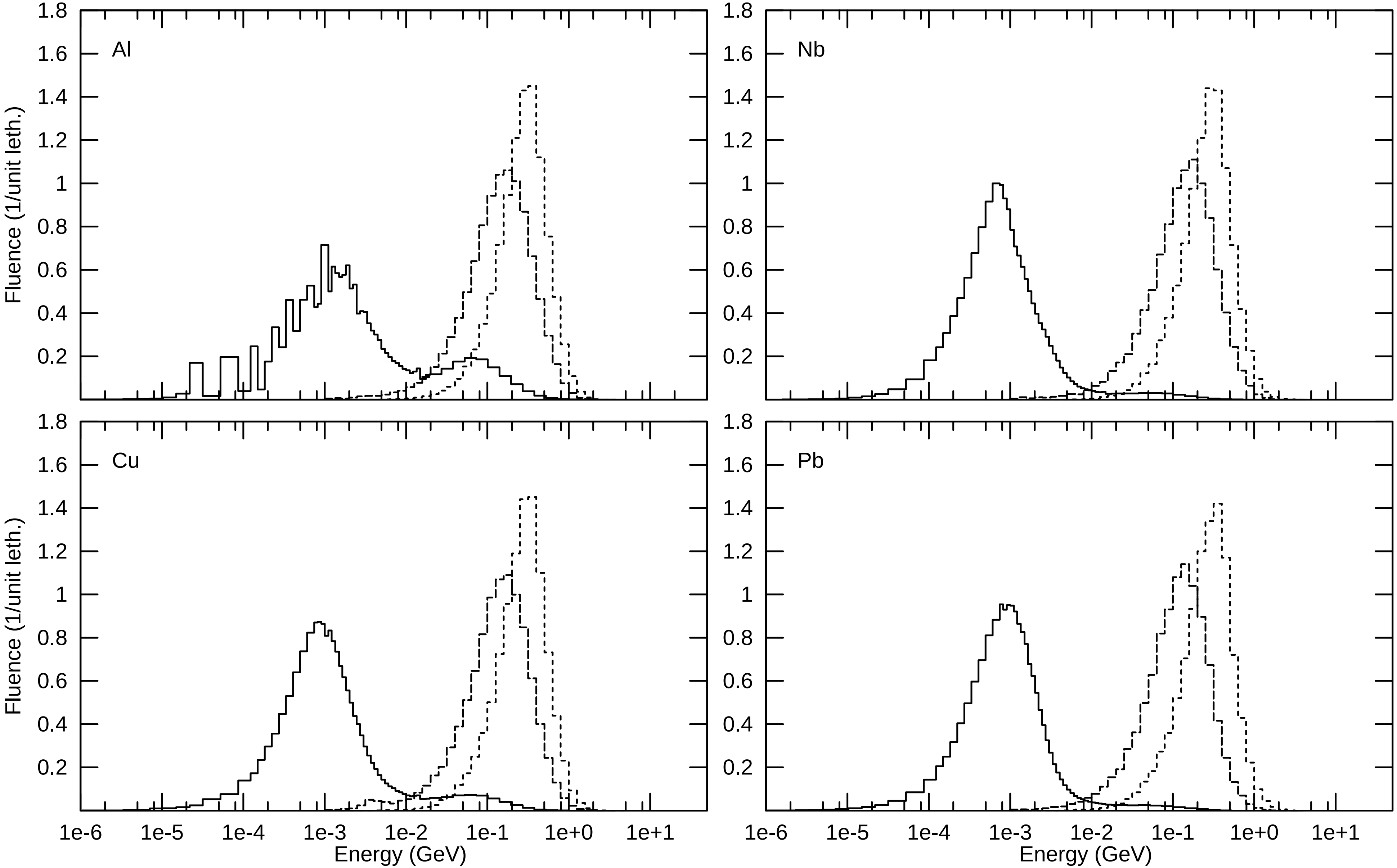

Fig. II.3: 30 GeV electron beam, Theta angle interval 40-50 deg
LINES: continuous - Neutrons, dashed - Protons, dotted - Charged pions

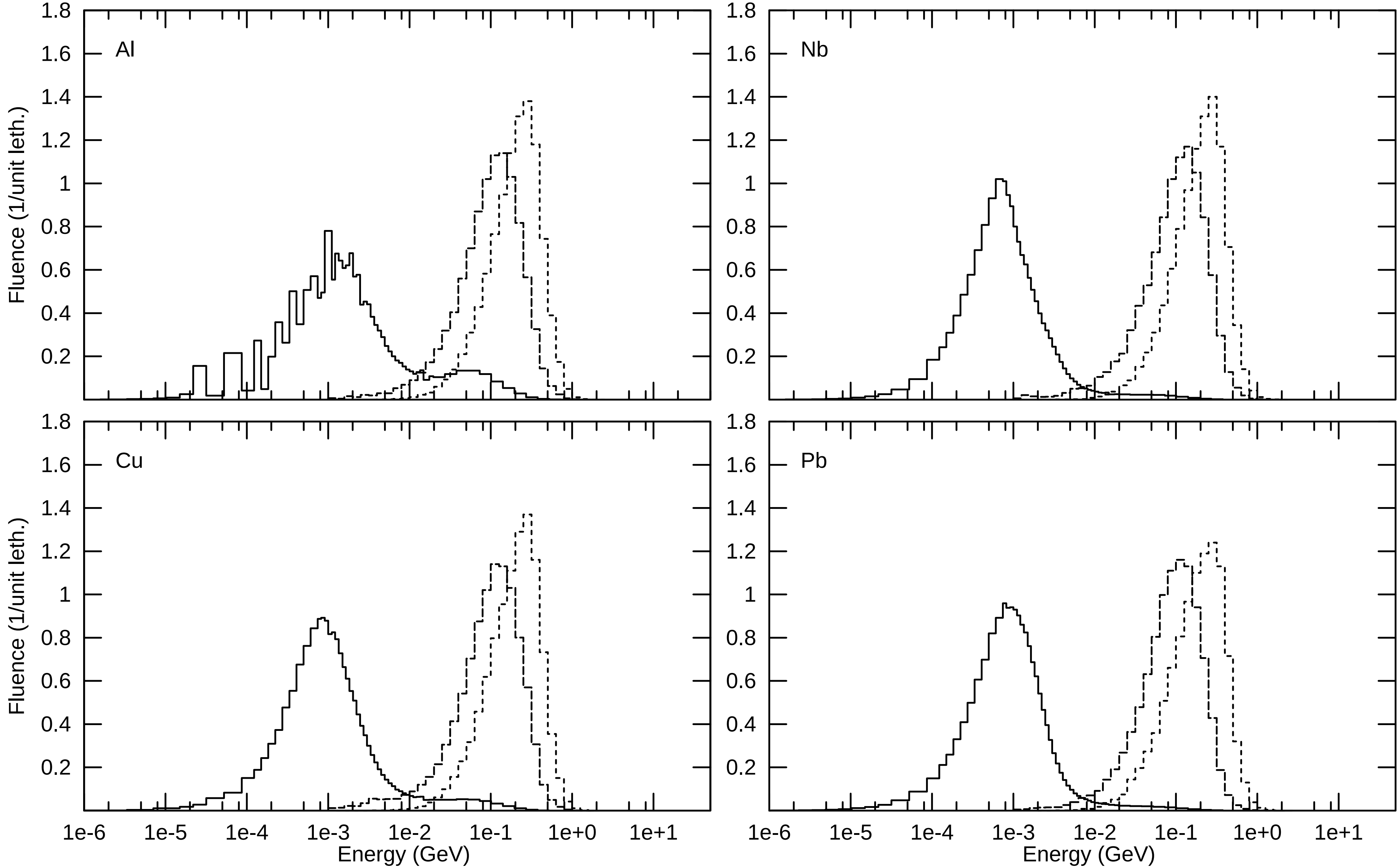

Fig. II.4: 30 GeV electron beam, Theta angle interval 60-70 deg
LINES: continuous - Neutrons, dashed - Protons, dotted - Charged pions

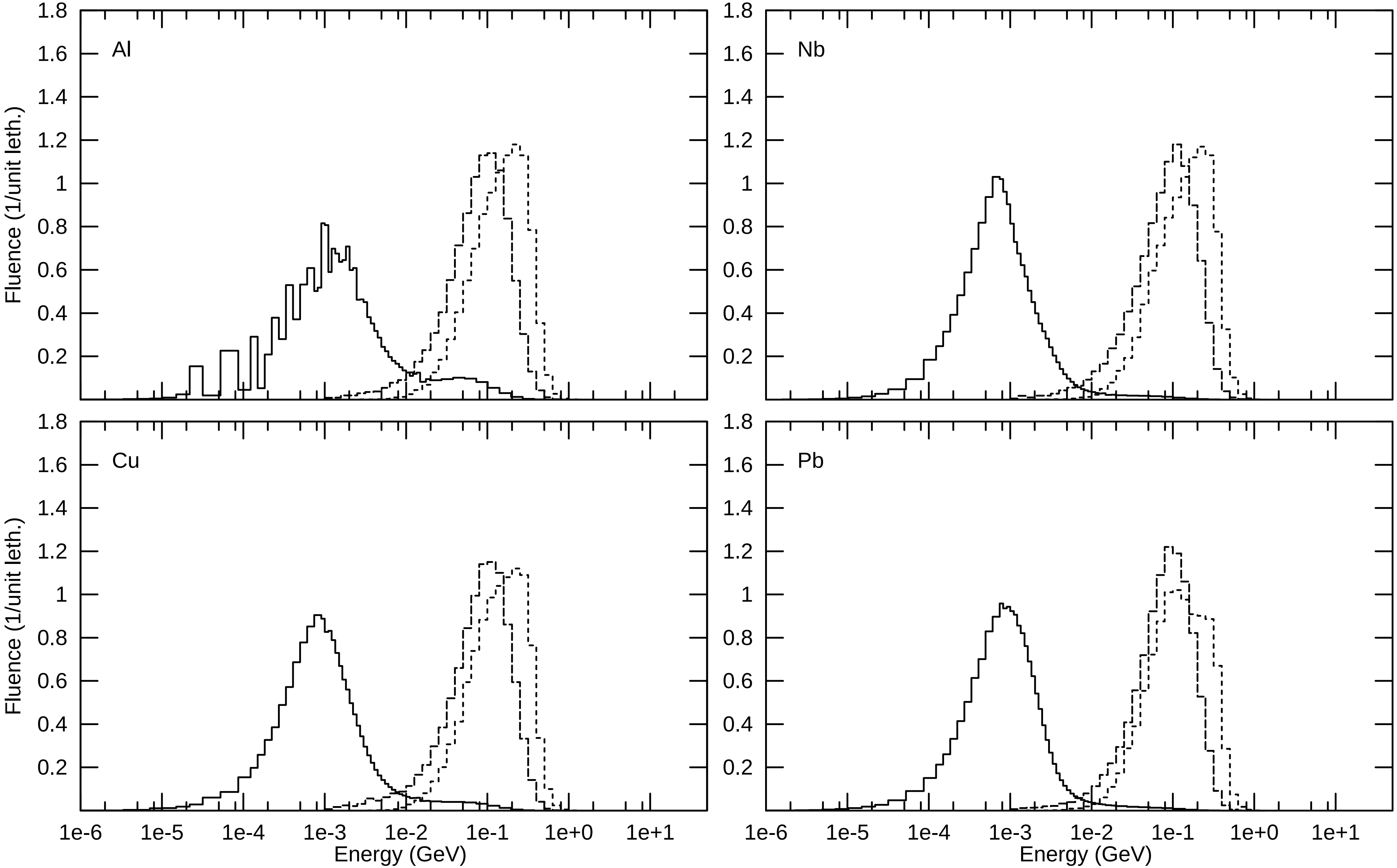

Fig. II.5: 30 GeV electron beam, Theta angle interval 80-100 deg
LINES: continuous - Neutrons, dashed - Protons, dotted - Charged pions

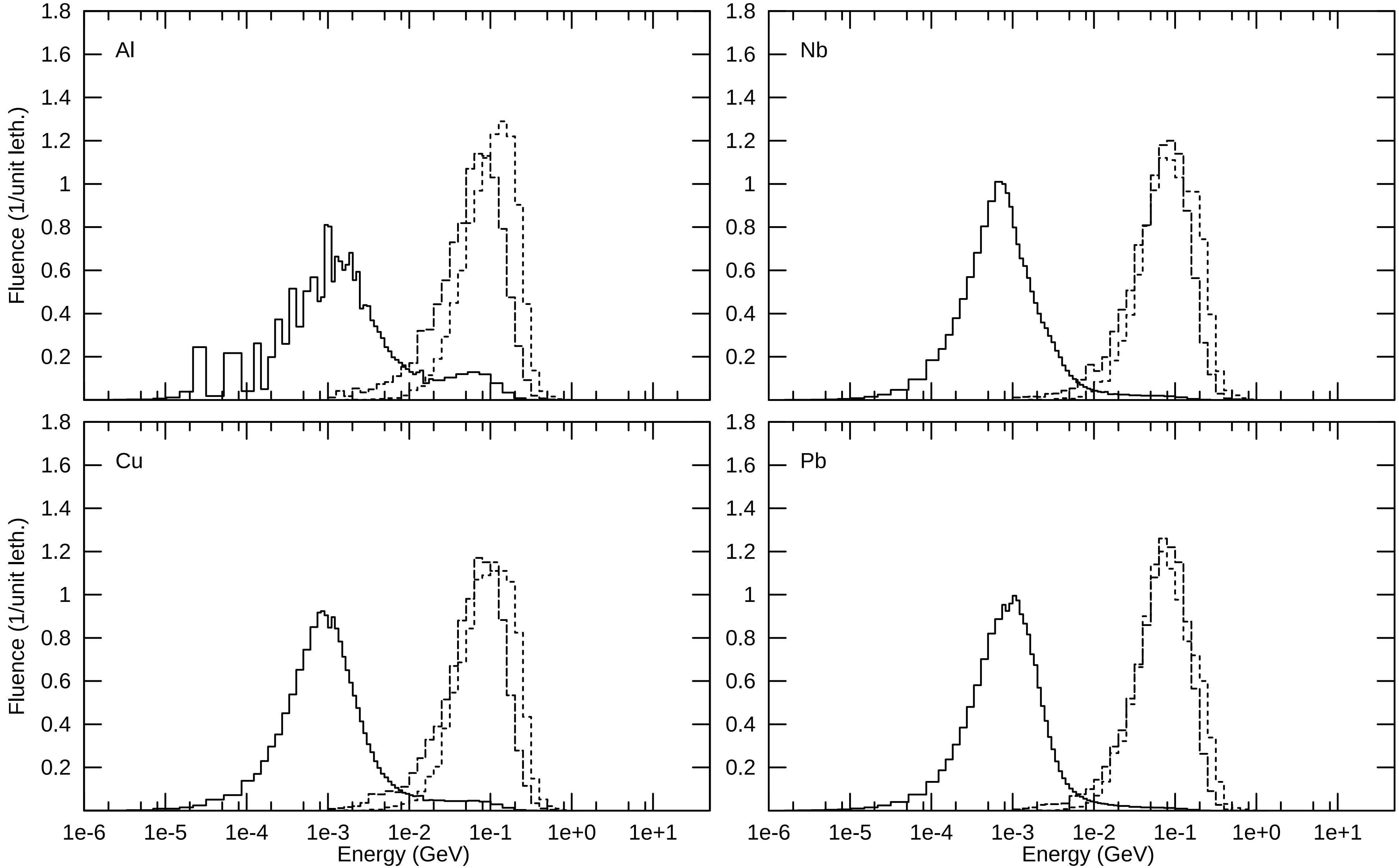

Fig. II.6: 30 GeV electron beam, Theta angle interval 140-160 deg

LINES: continuous - Neutrons, dashed - Protons, dotted - Charged pions

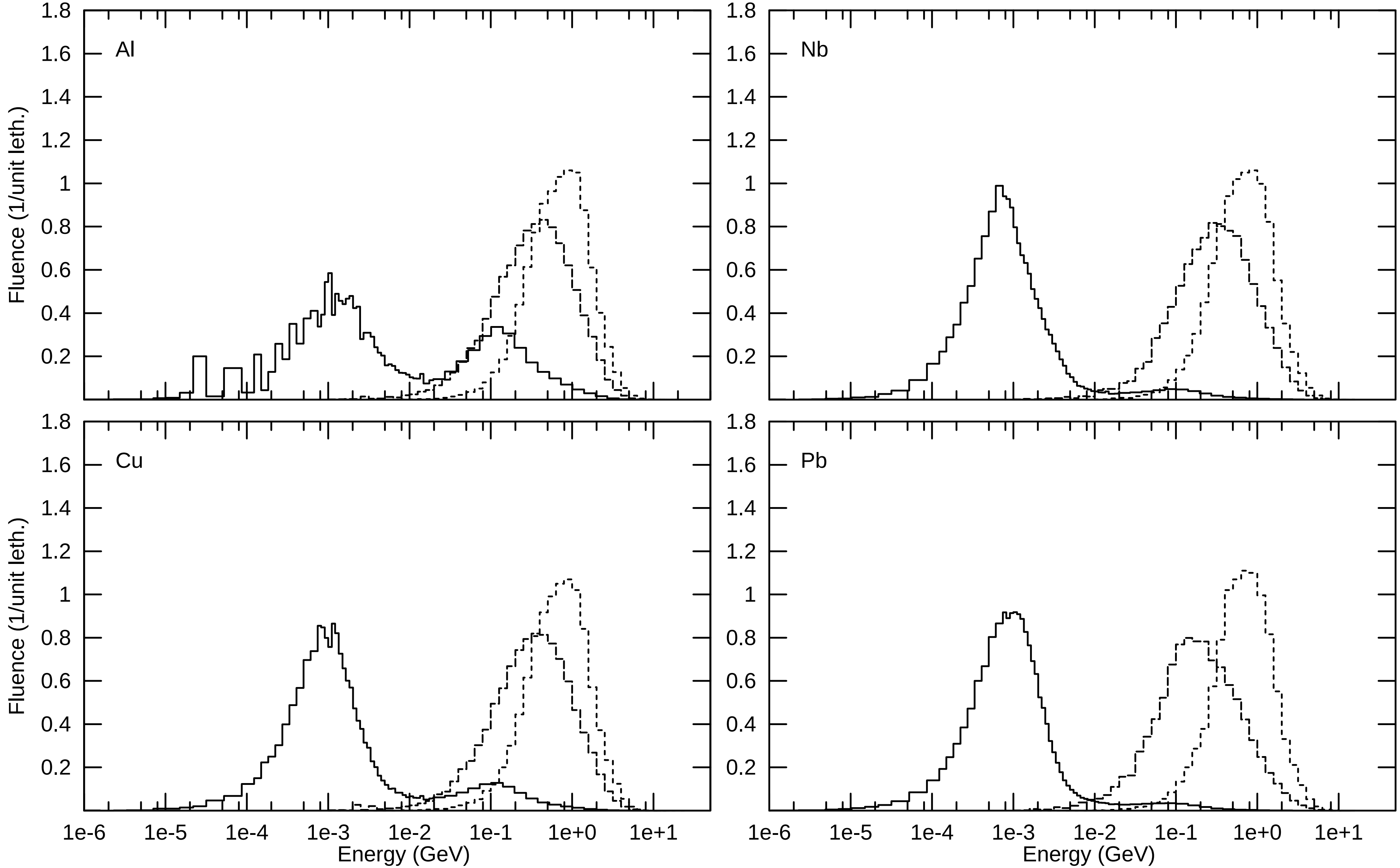

Fig. III.1: 250 GeV electron beam, Theta angle interval 10-20 deg
LINES: continuous - Neutrons, dashed - Protons, dotted - Charged pions

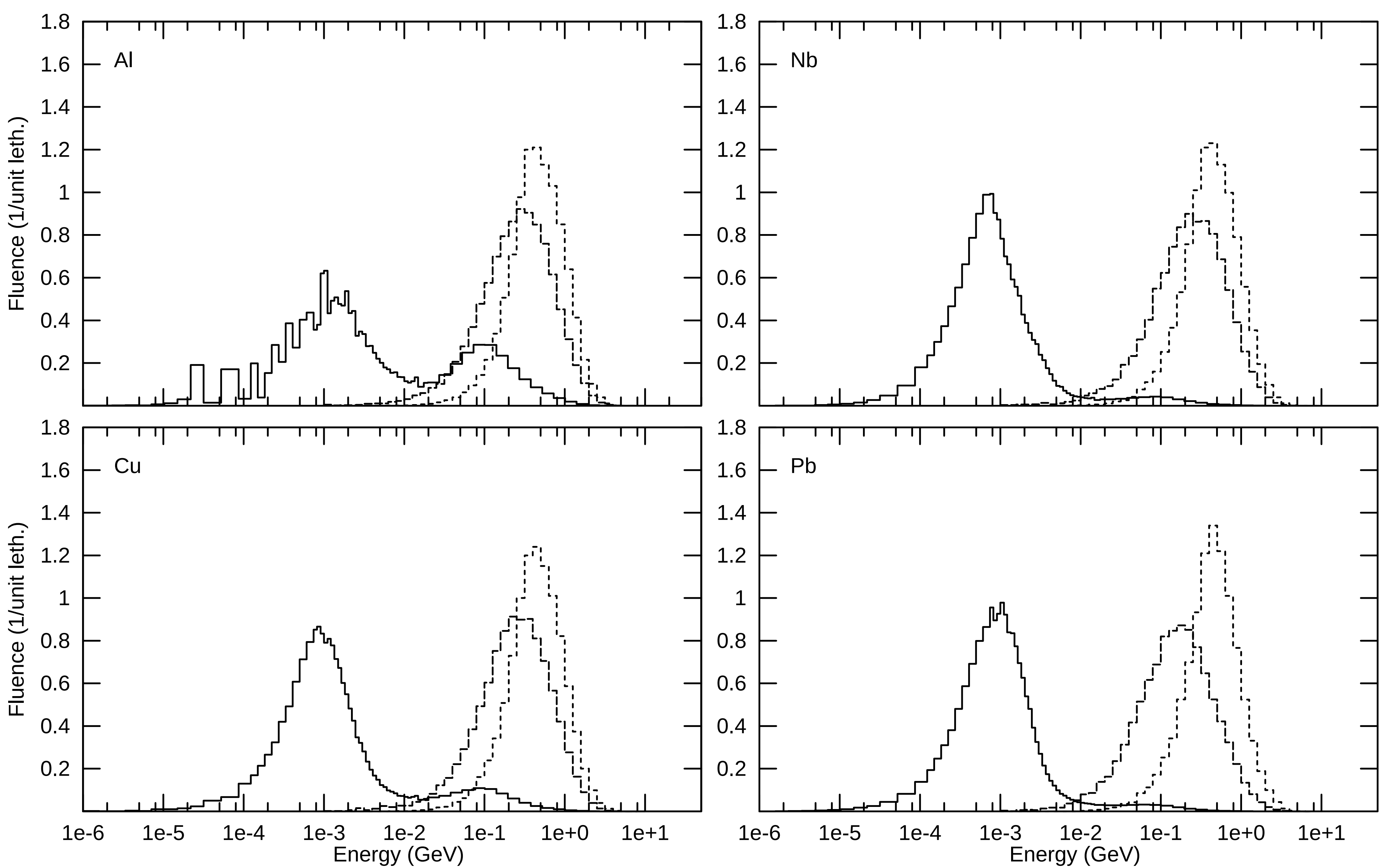

Fig. III.2: 250 GeV electron beam, Theta angle interval 20-30 deg
LINES: continuous - Neutrons, dashed - Protons, dotted - Charged pions

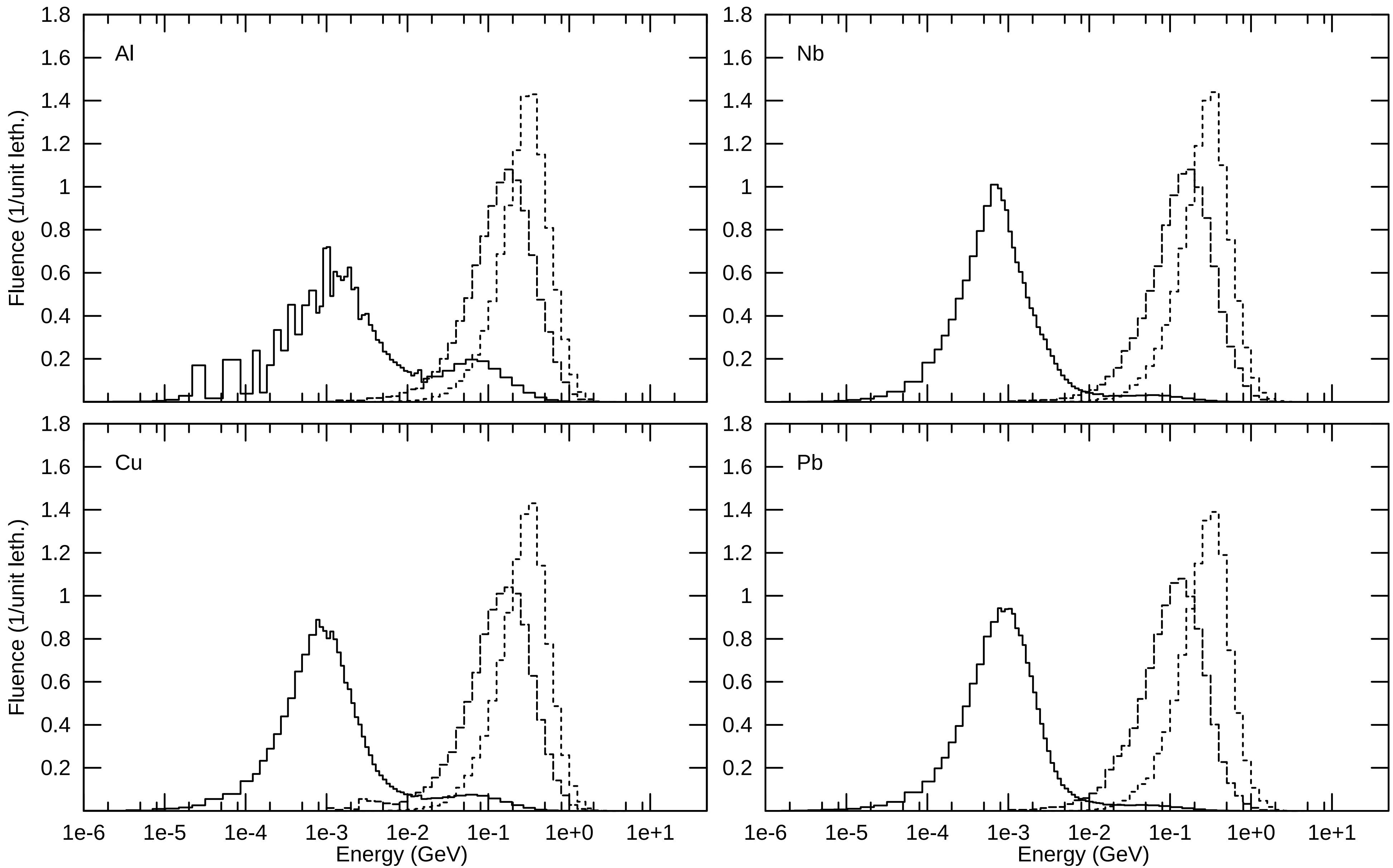

Fig. III.3: 250 GeV electron beam, Theta angle interval 40-50 deg
LINES: continuous - Neutrons, dashed - Protons, dotted - Charged pions

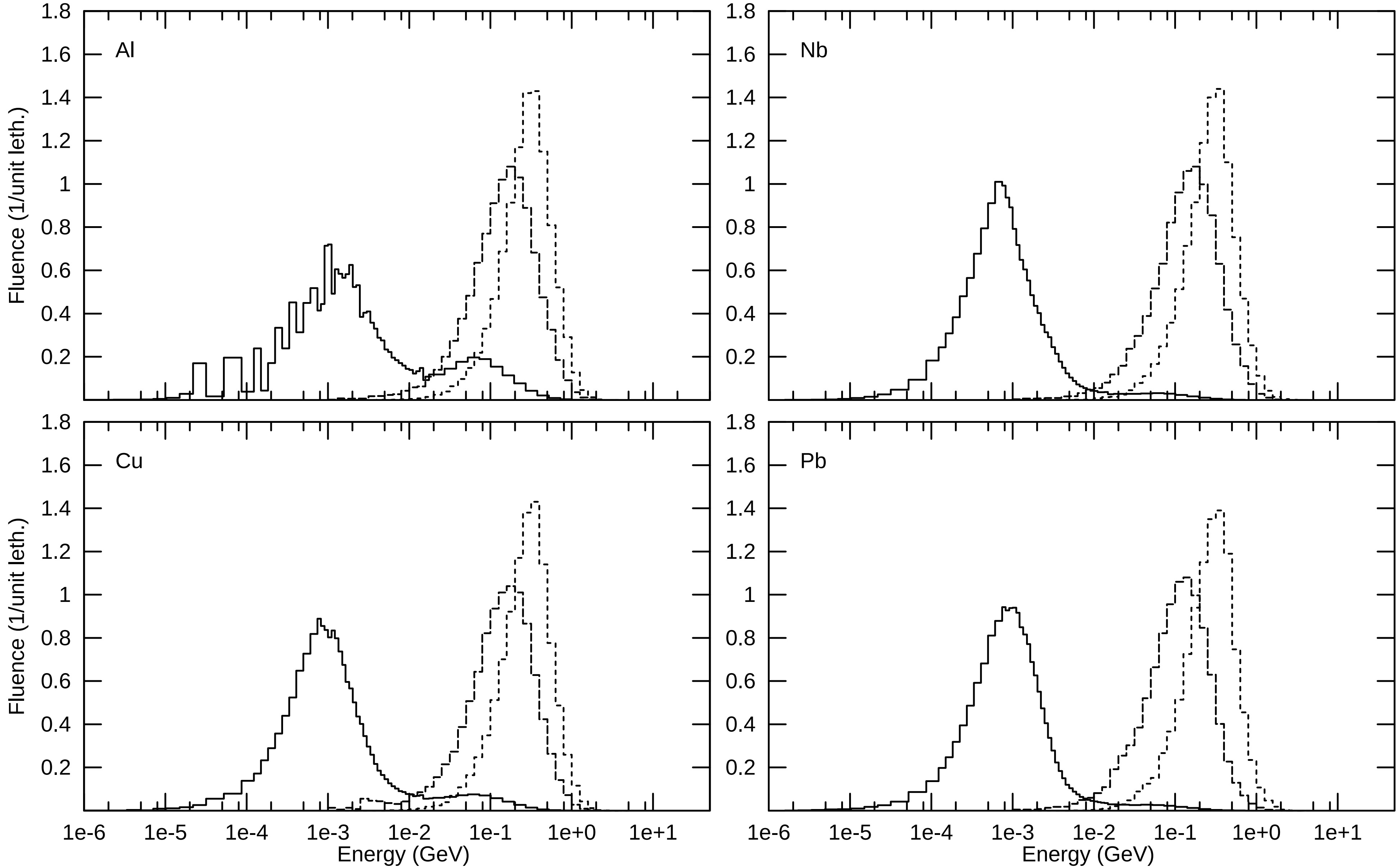

Fig. III.3: 250 GeV electron beam, Theta angle interval 40-50 deg

LINES: continuous - Neutrons, dashed - Protons, dotted - Charged pions

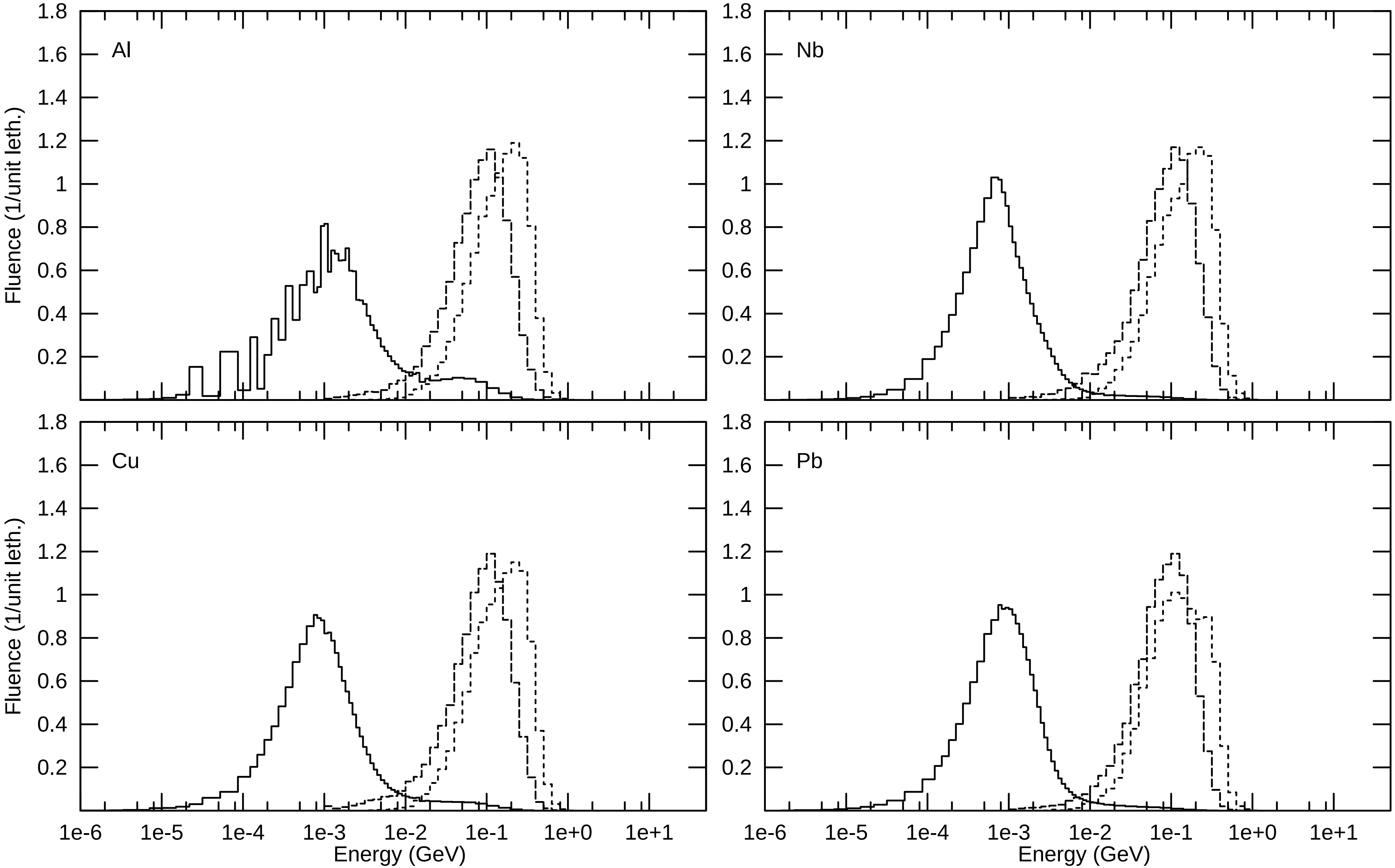

Fig. III.5: 250 GeV electron beam, Theta angle interval 80-100 deg
LINES: continuous - Neutrons, dashed - Protons, dotted - Charged pions

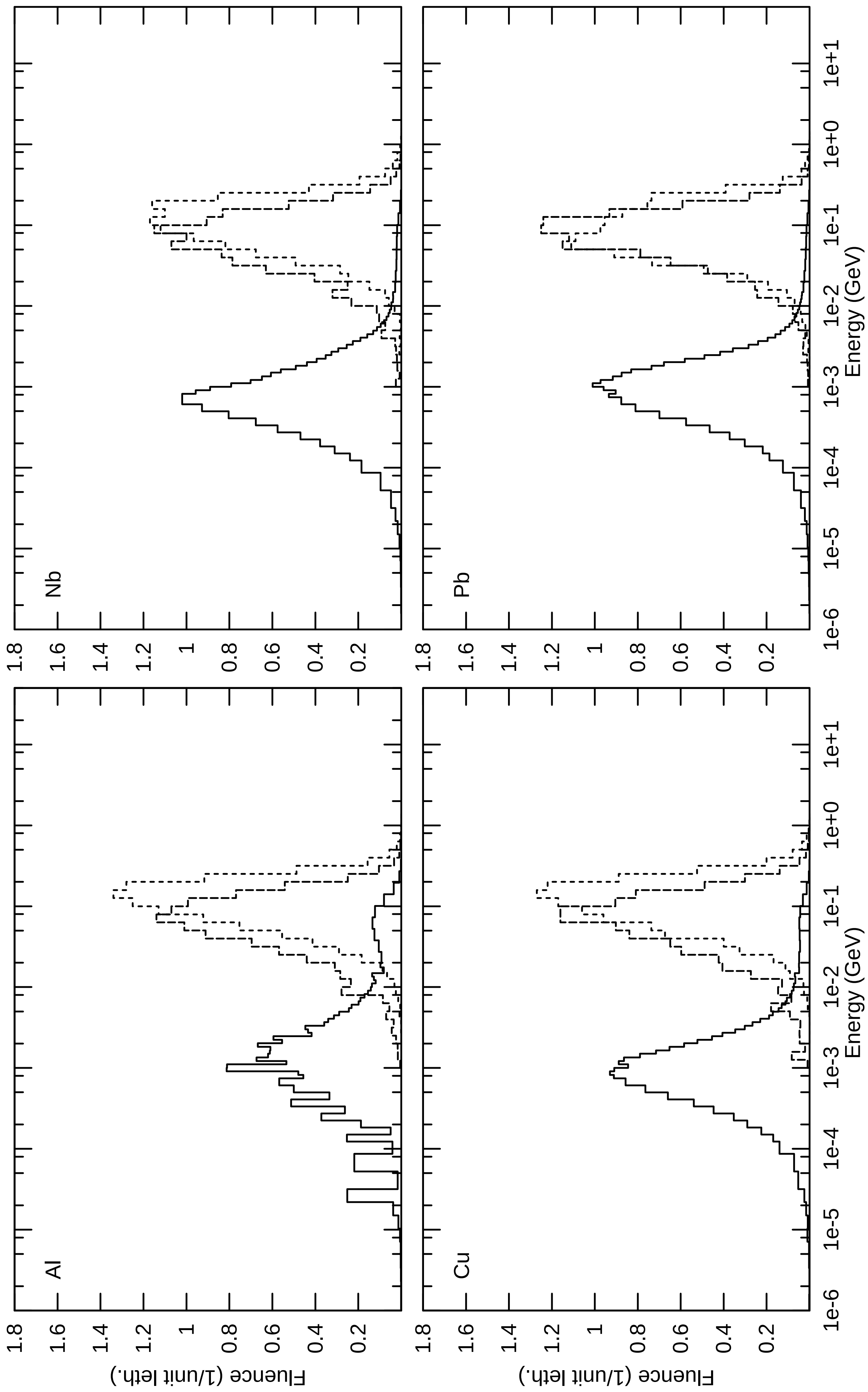

Fig. III.6: 250 GeV electron beam, Theta angle interval 140-160 deg

LINES: continuous - Neutrons, dashed - Protons, dotted - Charged pions

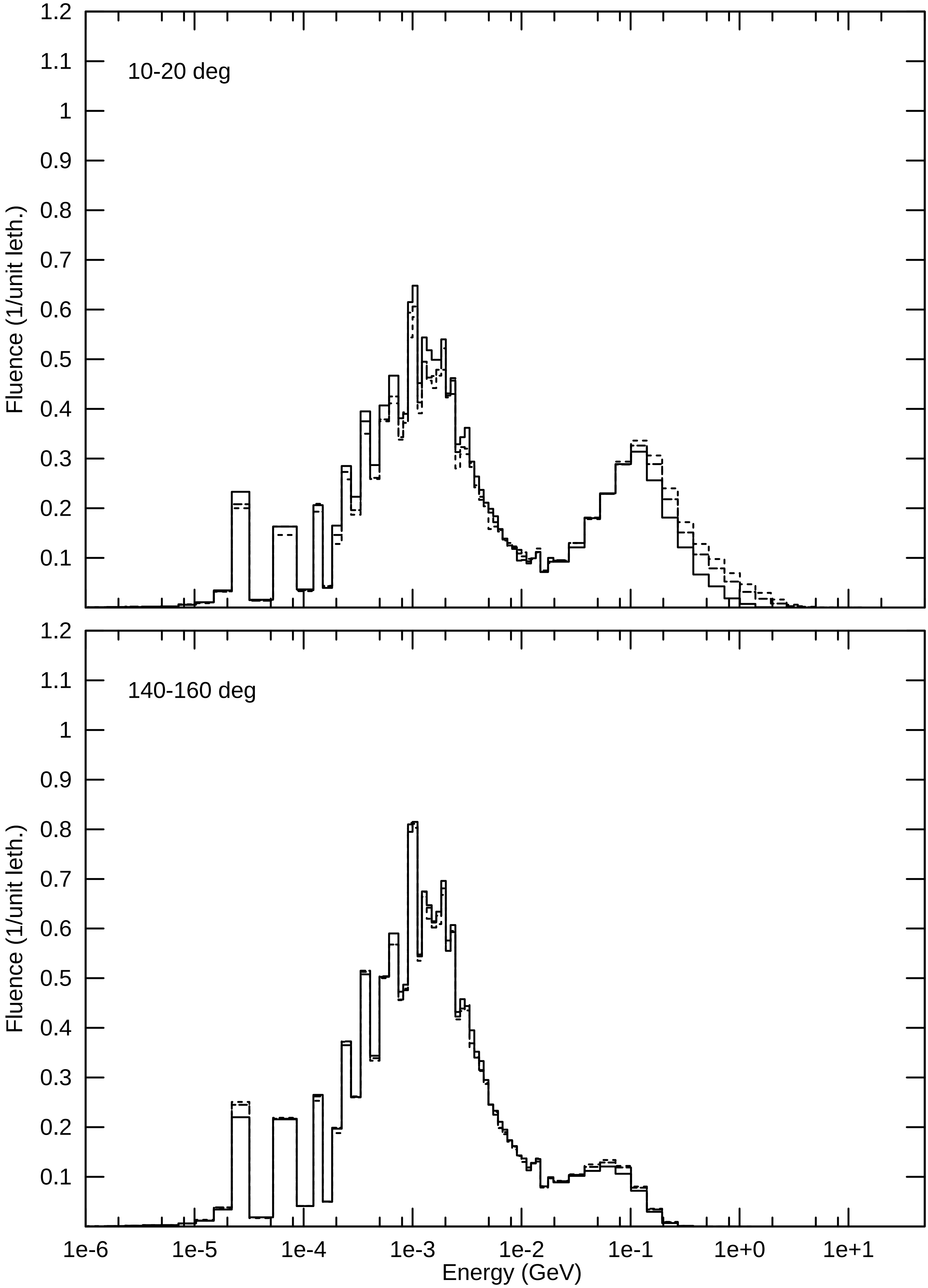

Fig. IV.1: Neutron spectra, Al target

LINES: continuous - 3 GeV, dashed - 30 GeV, dotted - 250 GeV

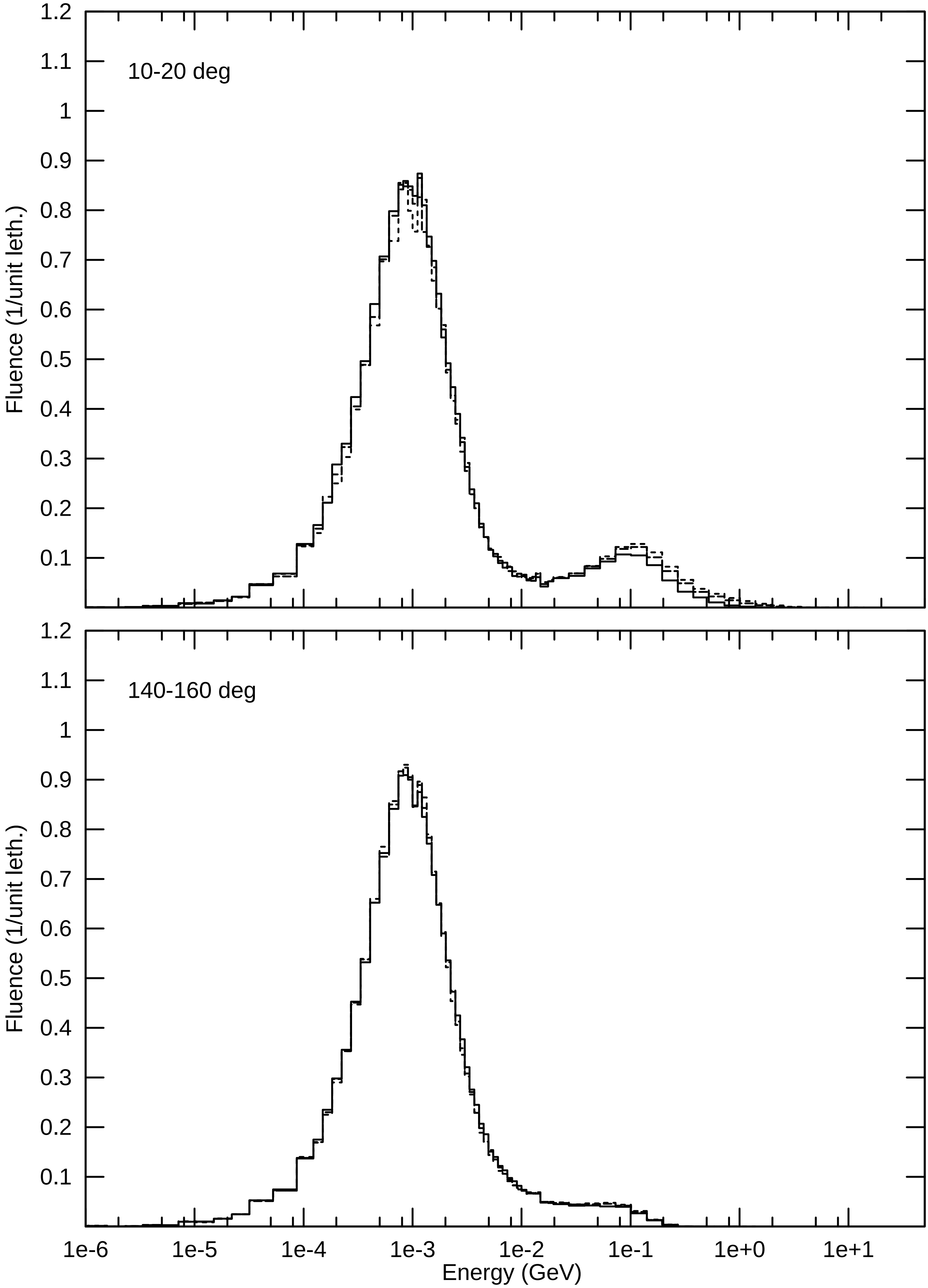

Fig. IV.2: Neutron spectra, Cu target

LINES: continuous - 3 GeV, dashed - 30 GeV, dotted - 250 GeV

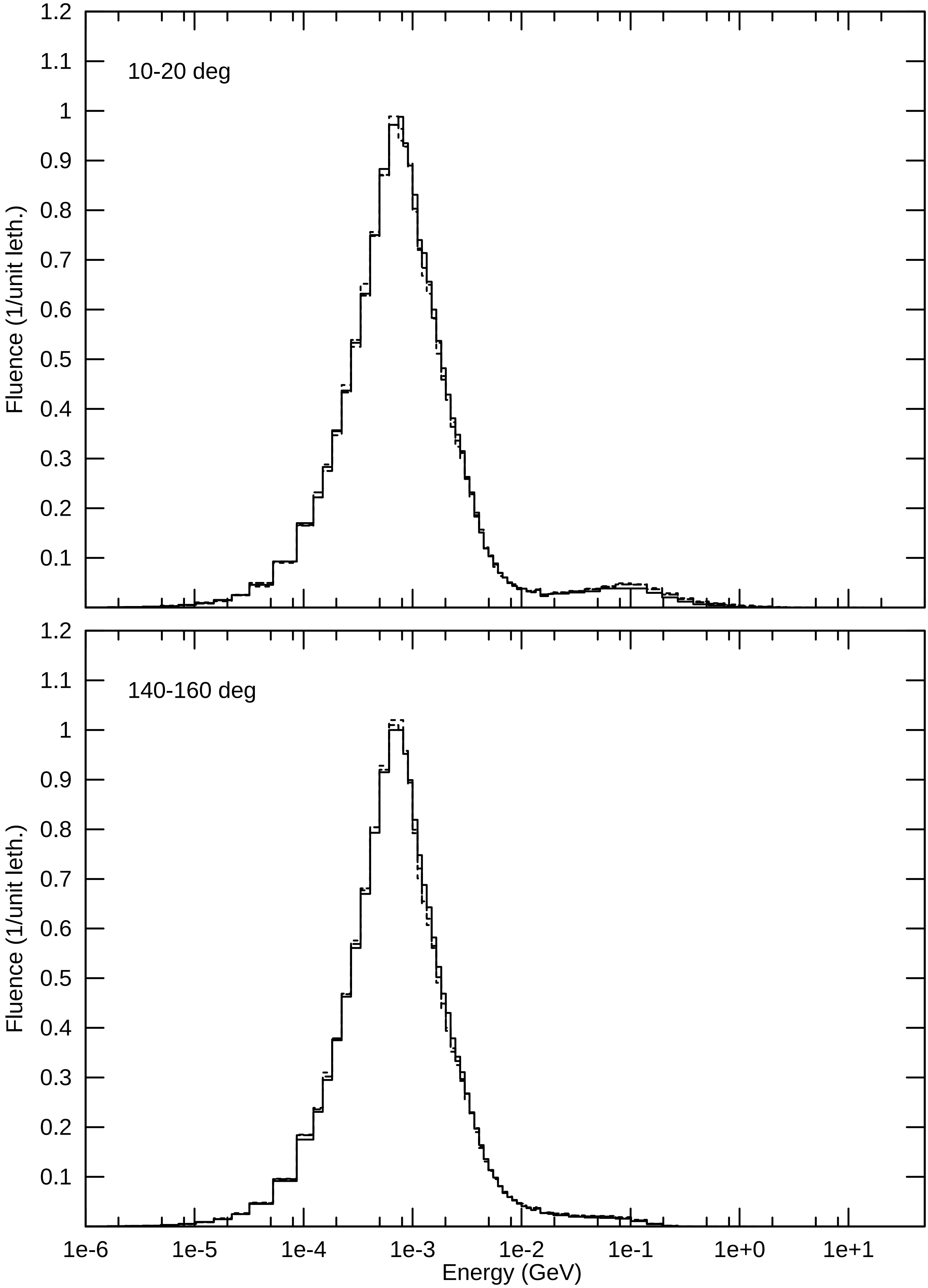

Fig. IV.3: Neutron spectra, Nb target

LINES: continuous - 3 GeV, dashed - 30 GeV, dotted - 250 GeV

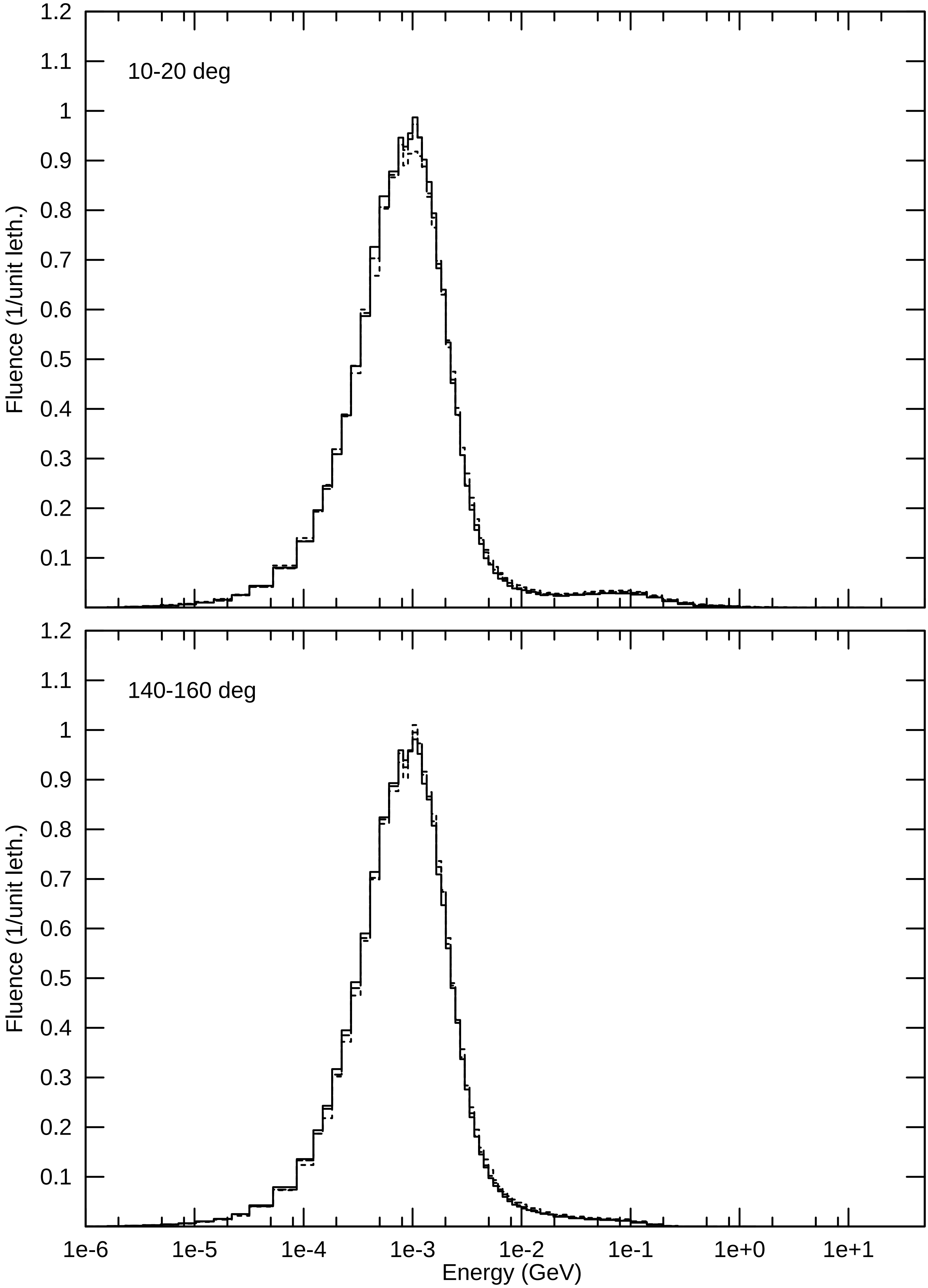

Fig. IV.4: Neutron spectra, Pb target

LINES: continuous - 3 GeV, dashed - 30 GeV, dotted - 250 GeV

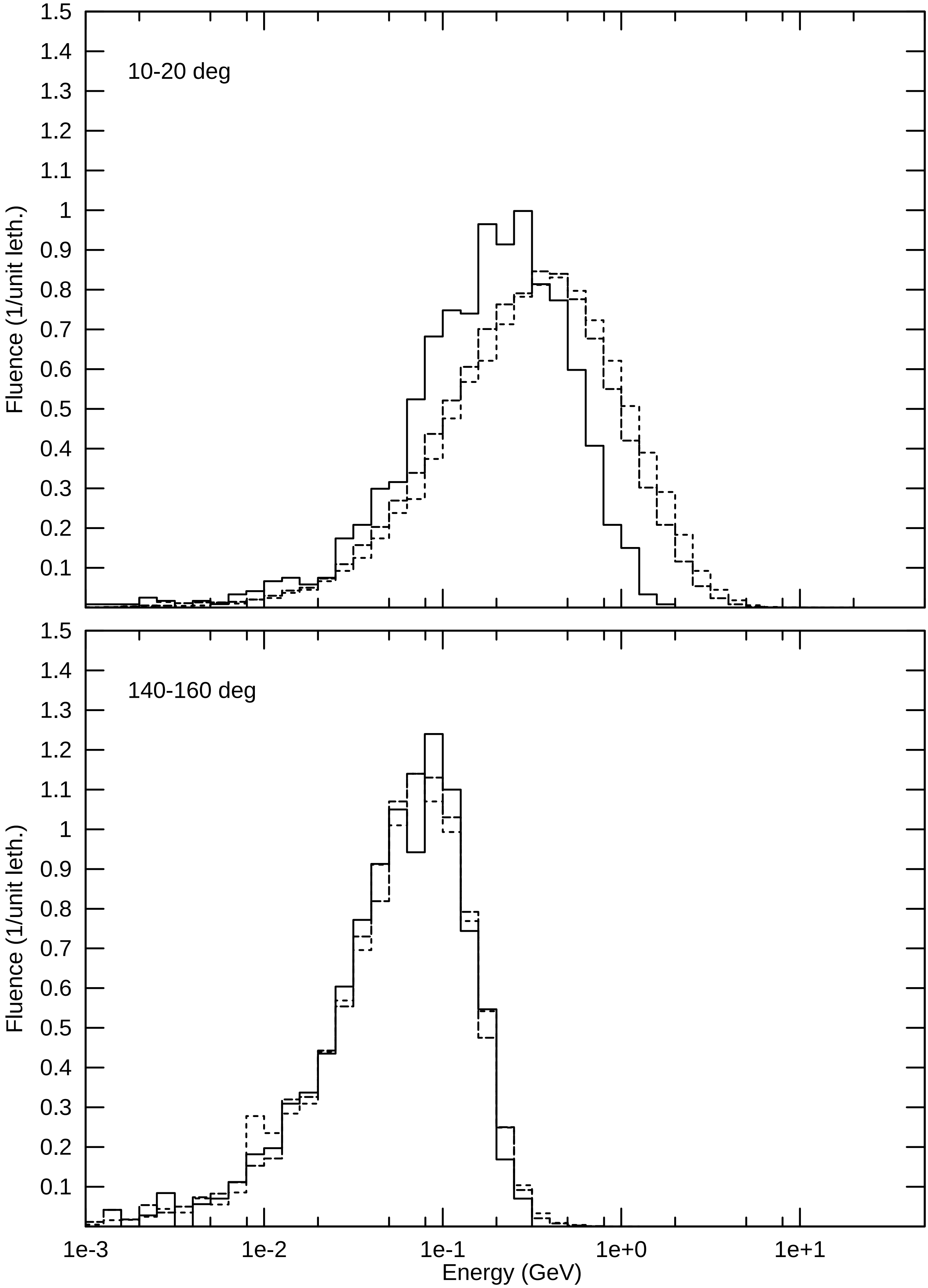

Fig. V.1: Proton spectra, Al target

LINES: continuous - 3 GeV, dashed - 30 GeV, dotted - 250 GeV

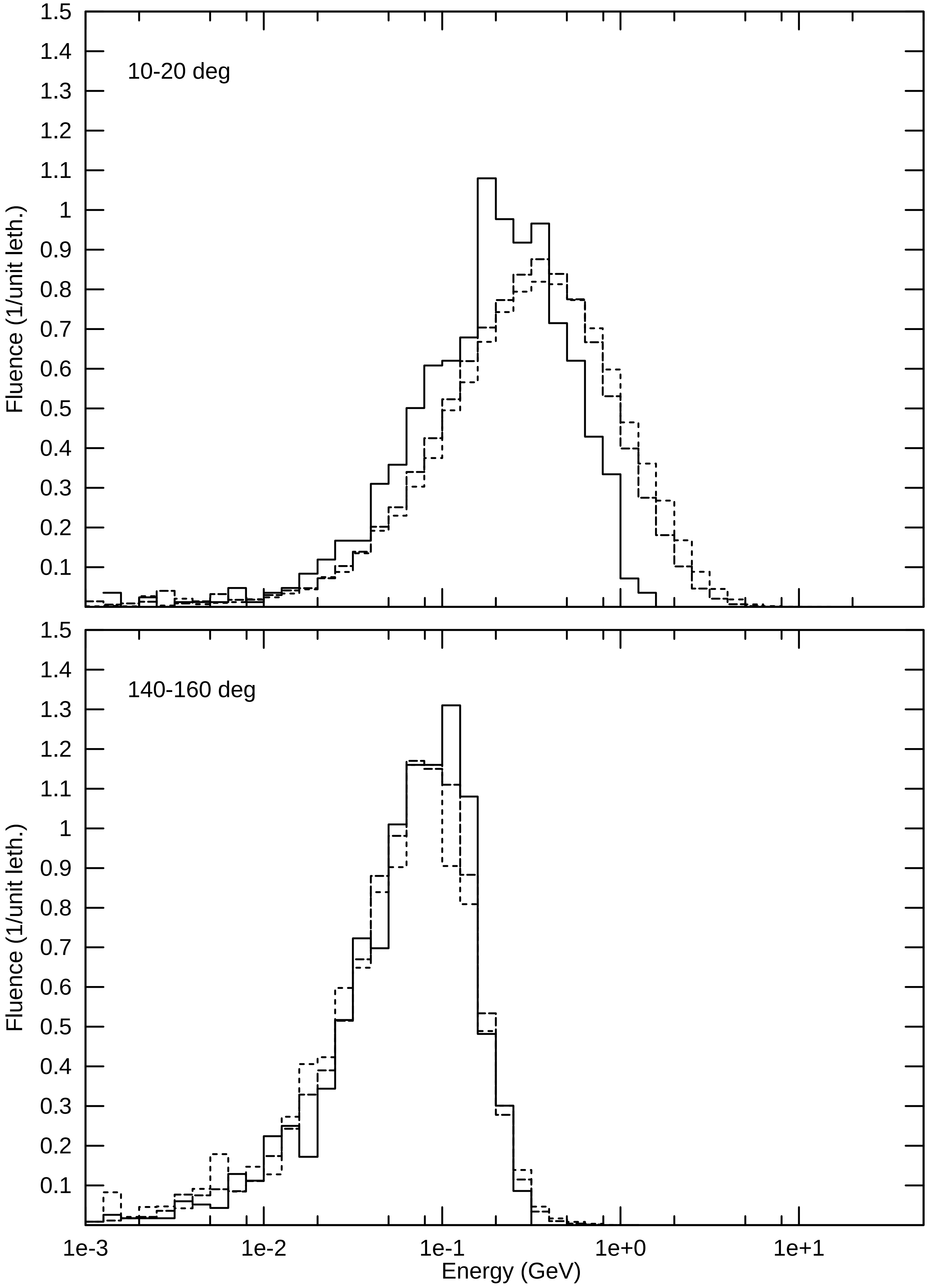

Fig. V.2: Proton spectra, Cu target

LINES: continuous - 3 GeV, dashed - 30 GeV, dotted - 250 GeV

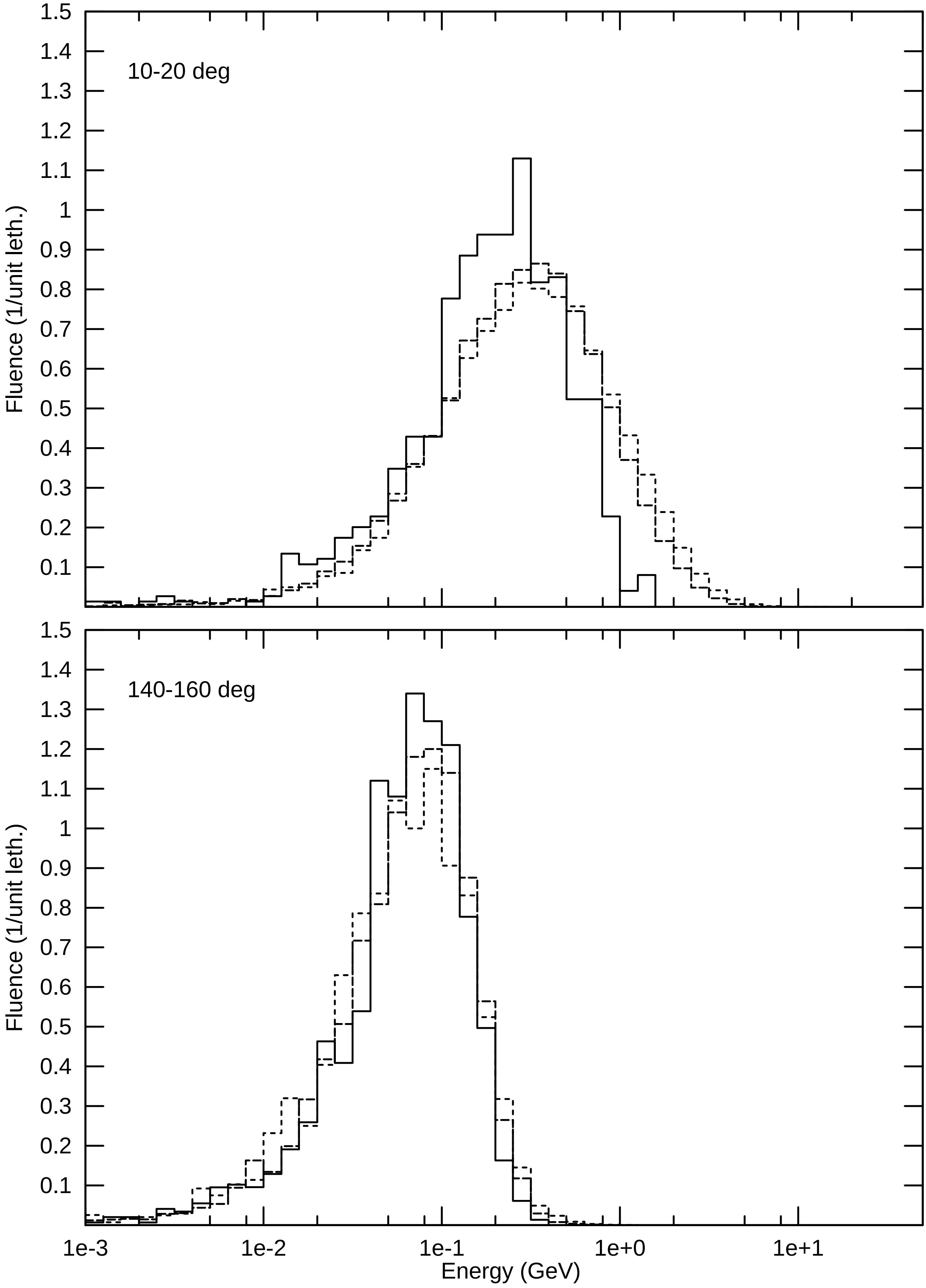

Fig. V.3: Proton spectra, Nb target

LINES: continuous - 3 GeV, dashed - 30 GeV, dotted - 250 GeV

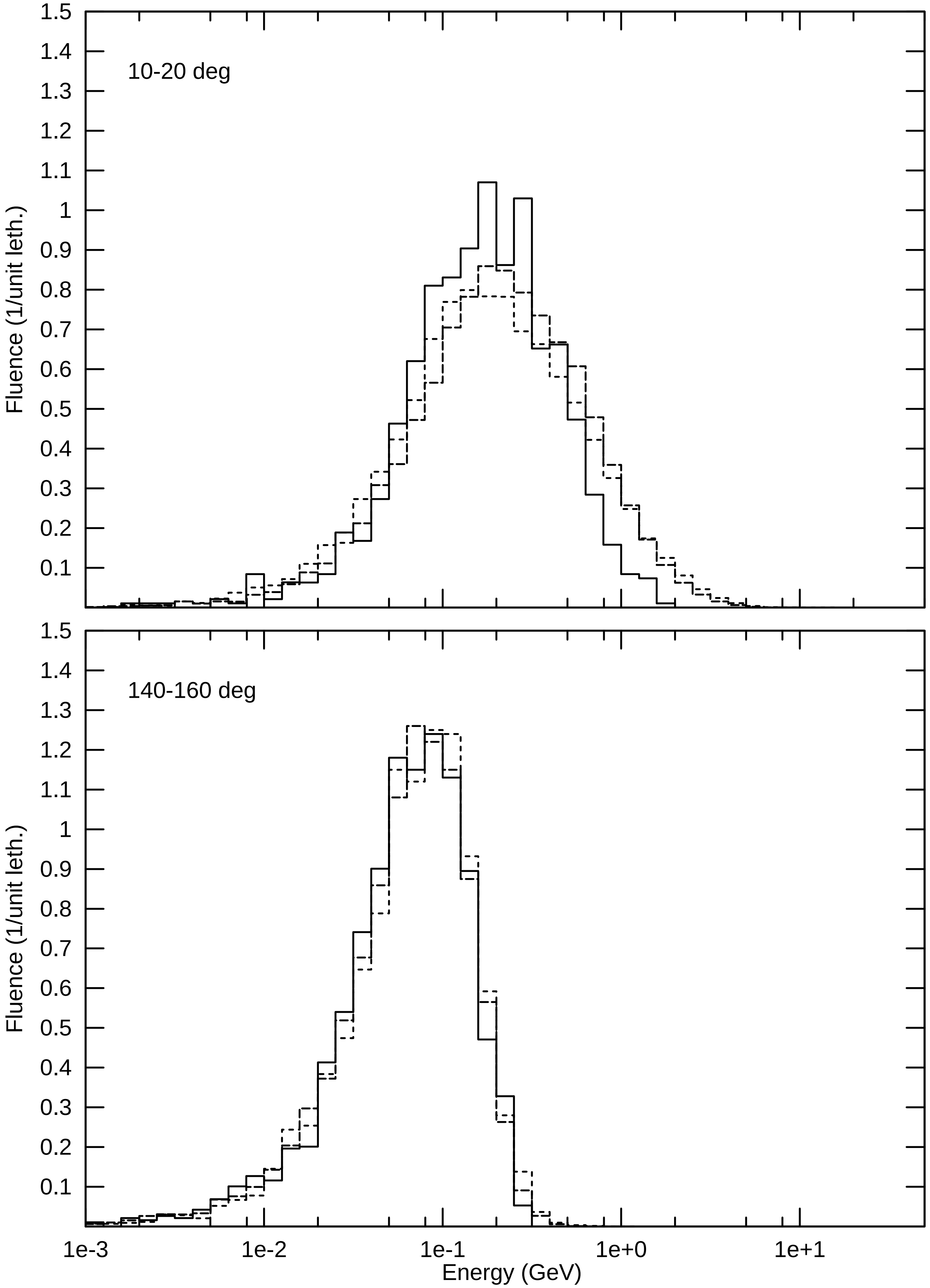

Fig. V.4: Proton spectra, Pb target

LINES: continuous - 3 GeV, dashed - 30 GeV, dotted - 250 GeV

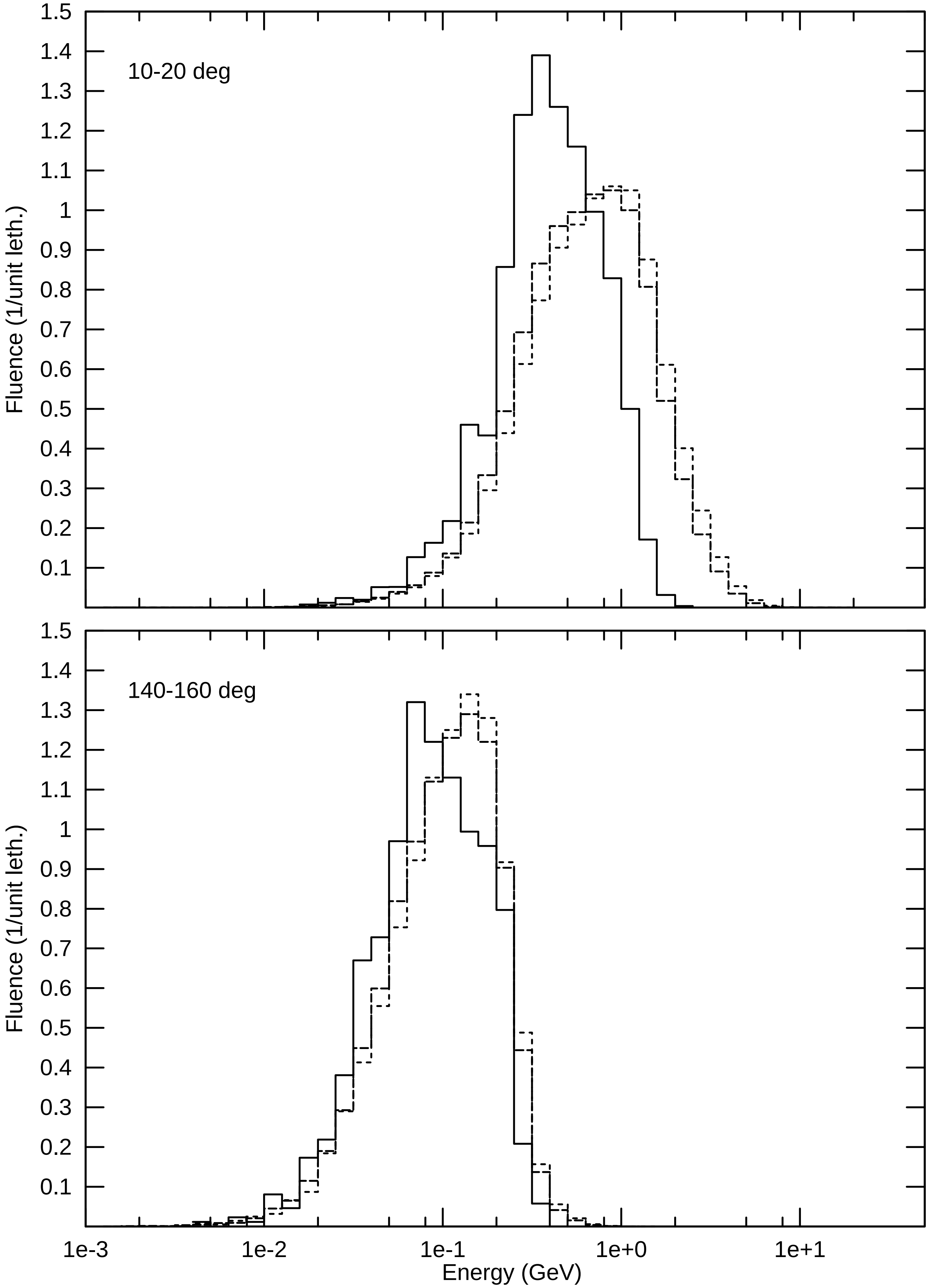

Fig. VI.1: Charged pions spectra, Al target

LINES: continuous - 3 GeV, dashed - 30 GeV, dotted - 250 GeV

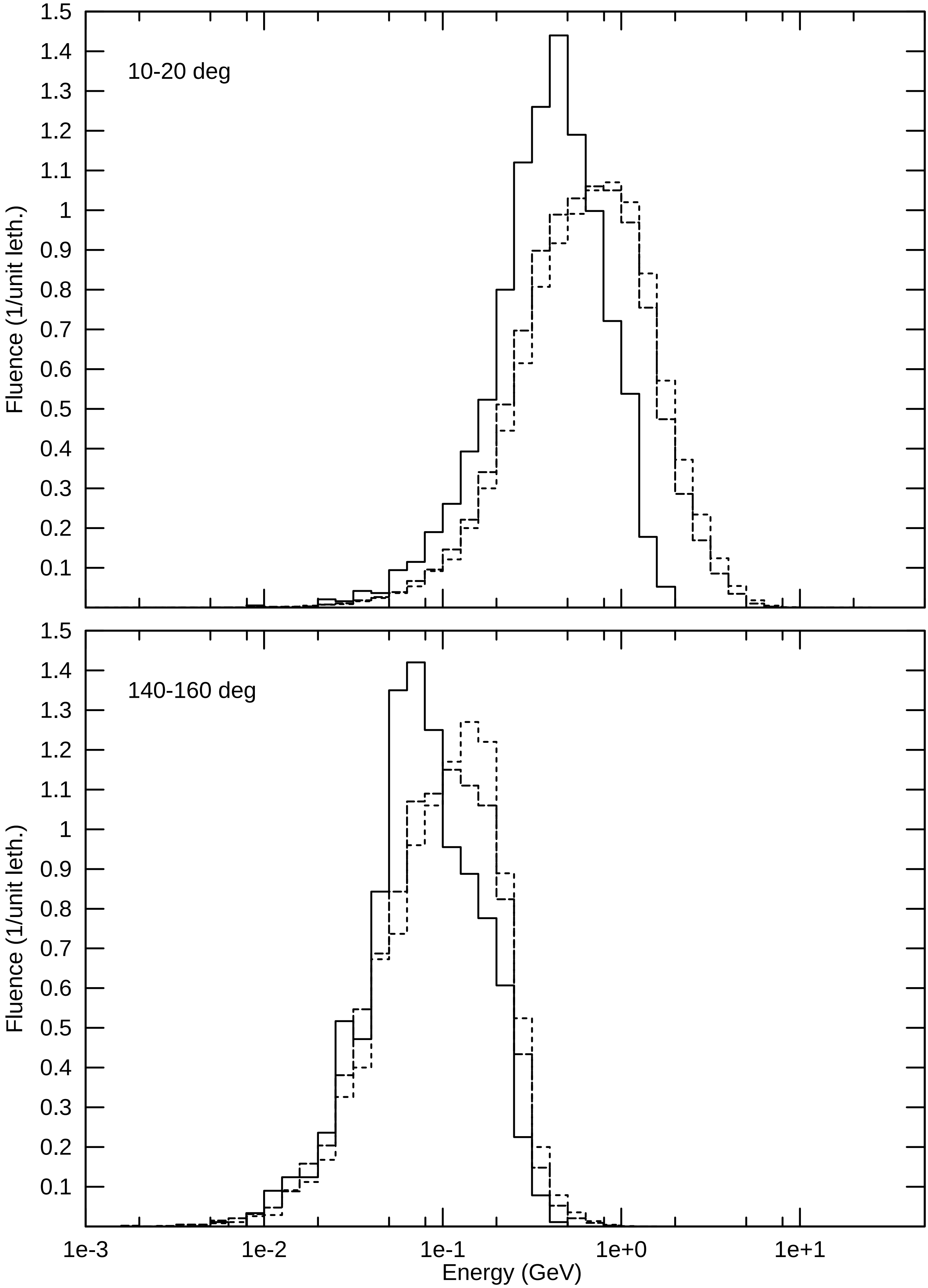

Fig. VI.2: Charged pions spectra, Cu target

LINES: continuous - 3 GeV, dashed - 30 GeV, dotted - 250 GeV

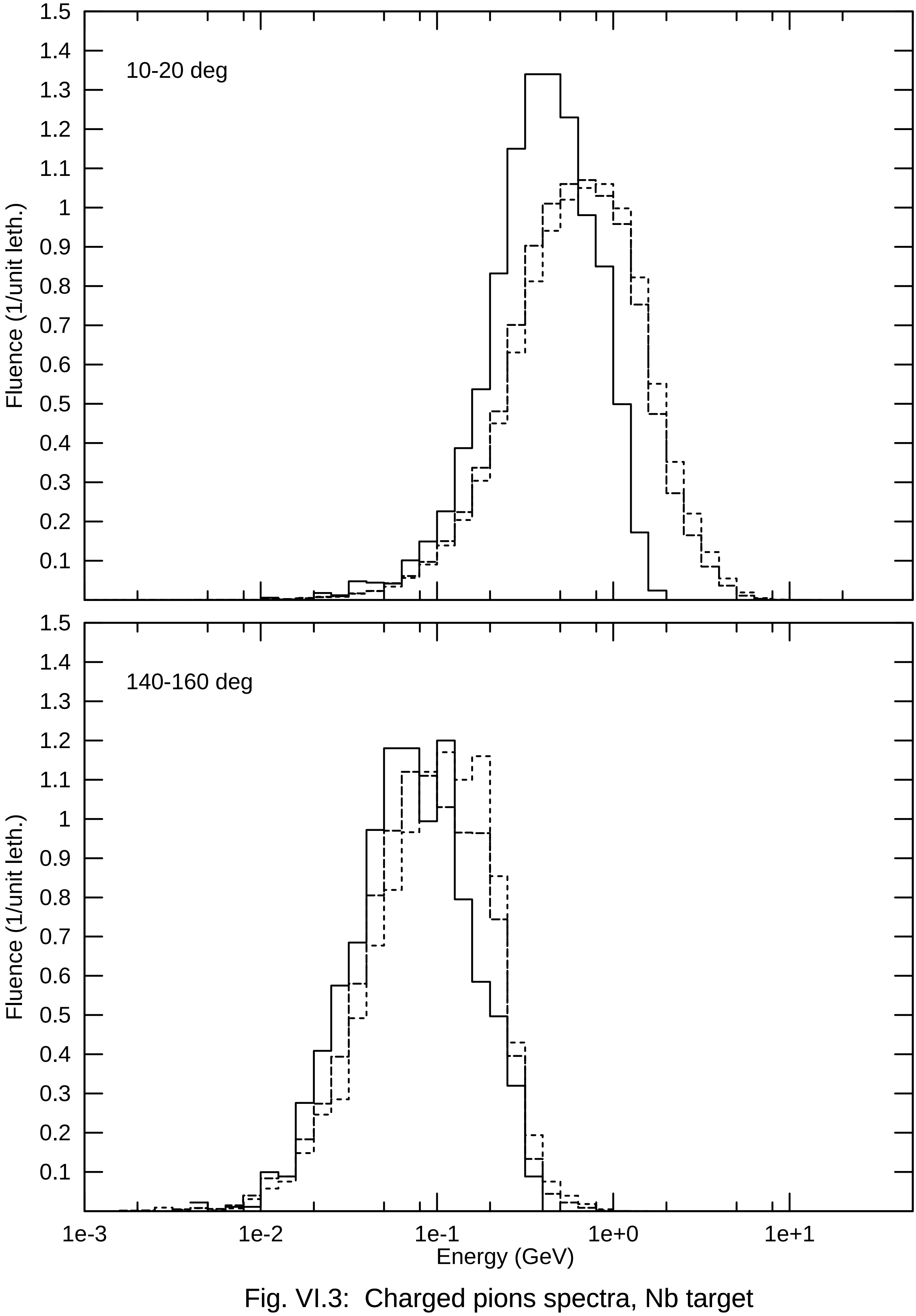

Fig. VI.3: Charged pions spectra, Nb target

LINES: continuous - 3 GeV, dashed - 30 GeV, dotted - 250 GeV

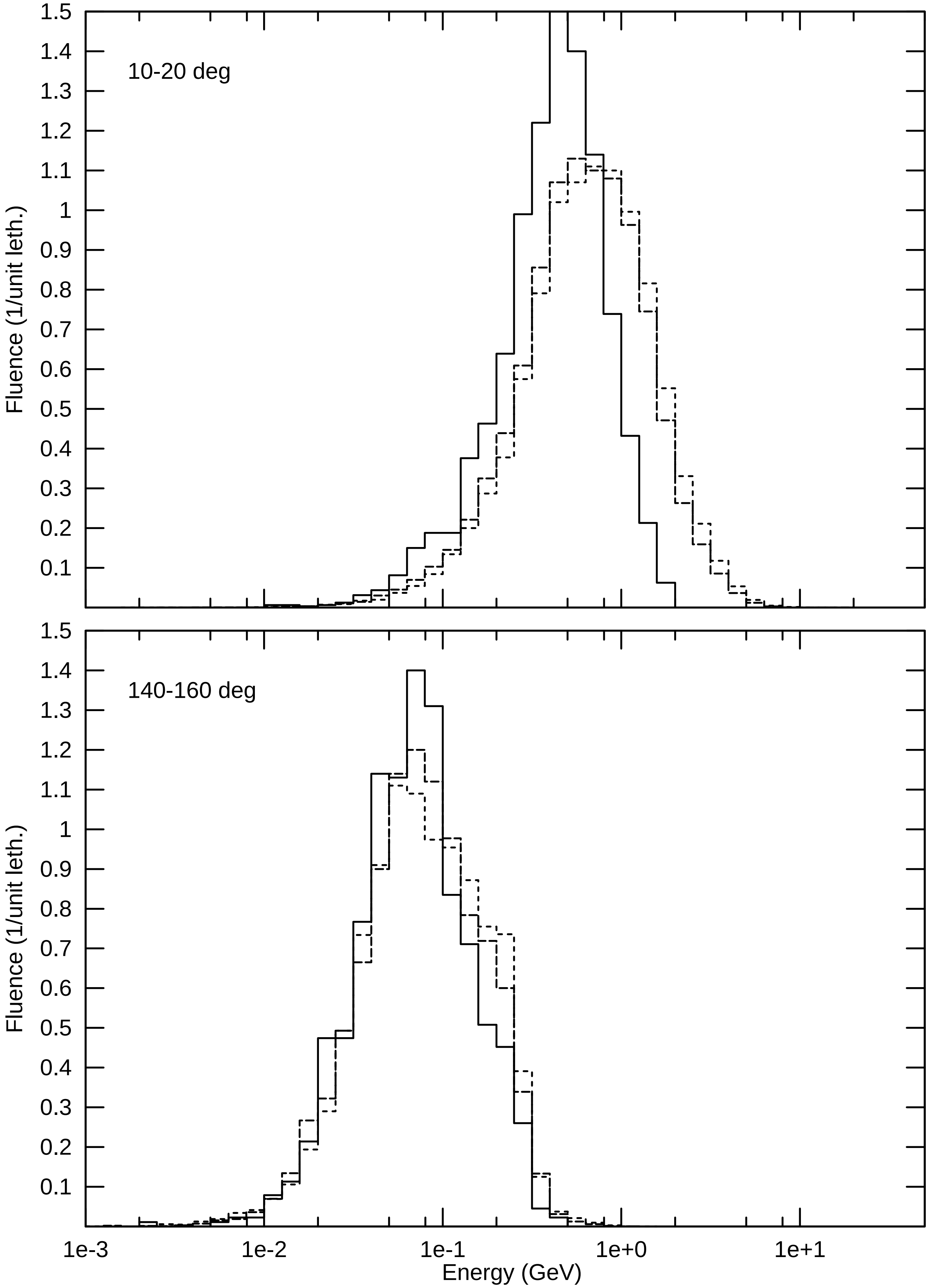

Fig. VI.4: Charged pions spectra, Pb target

LINES: continuous - 3 GeV, dashed - 30 GeV, dotted - 250 GeV